

AD-A020 356

INDUCED SIDE FORCES ON BODIES OF REVOLUTION AT HIGH  
ANGLE OF ATTACK

Andrew B. Wardlaw, Jr.. et al

Naval Surface Weapons Center  
White Oak Laboratory, Silver Spring, Maryland

1 November 1975

DISTRIBUTED BY:

**NTIS**

National Technical Information Service  
U. S. DEPARTMENT OF COMMERCE

## **DISCLAIMER NOTICE**

**THIS DOCUMENT IS BEST QUALITY  
PRACTICABLE. THE COPY FURNISHED  
TO DTIC CONTAINED A SIGNIFICANT  
NUMBER OF PAGES WHICH DO NOT  
REPRODUCE LEGIBLY.**

/

NSWC/WOL/TR 75-176

# NSWC

## TECHNICAL REPORT

WHITE OAK LABORATORY

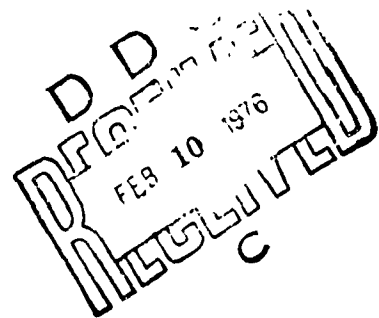
INDUCED SIDE FORCES ON BODIES OF REVOLUTION AT HIGH ANGLE OF ATTACK

BY  
Andrew B. Wardlaw, Jr.  
Alfred M. Morrison

1 NOVEMBER 1975

NAVAL SURFACE WEAPONS CENTER  
WHITE OAK LABORATORY  
SILVER SPRING, MARYLAND 20910

- Approved for public release; distribution unlimited



NAVAL SURFACE WEAPONS CENTER  
WHITE OAK, SILVER SPRING, MARYLAND 20910

Reproduced by  
NATIONAL TECHNICAL  
INFORMATION SERVICE  
U.S. Department of Commerce  
Springfield, VA 22151

ADA020356

UNCLASSIFIED

SECURITY CLASSIFICATION OF THIS PAGE (When Data Entered)

REPORT DOCUMENTATION PAGE		READ INSTRUCTIONS BEFORE COMPLETING FORM
1 REPORT NUMBER NSWC/WOL/TR 75-176	2 GOVT ACCESSION NO.	3 RECIPIENT'S CATALOG NUMBER
4 TITLE (and Subtitle) INDUCED SIDE FORCES ON BODIES OF REVOLUTION AT HIGH ANGLE OF ATTACK		5 TYPE OF REPORT & PERIOD COVERED
		6 PERFORMING ORG. REPORT NUMBER
7 AUTHOR(s) Andrew B. Wardlaw, Jr. Alfred M. Morrison		8 CONTRACT OR GRANT NUMBER(s)
9 PERFORMING ORGANIZATION NAME AND ADDRESS Naval Surface Weapons Center White Oak Laboratory White Oak, Silver Spring, Maryland 20910		10 PROGRAM ELEMENT, PROJECT, TASK AREA & WORK UNIT NUMBERS  A320-0000/WF32-322-202
11 CONTROLLING OFFICE NAME AND ADDRESS		12 REPORT DATE 1 November 1975
		13 NUMBER OF PAGES 41
14 MONITORING AGENCY NAME & ADDRESS (if different from Controlling Office)		15 SECURITY CLASS. (of this report)  UNCLASSIFIED
		15a. DECLASSIFICATION/DOWNGRADING SCHEDULE
16 DISTRIBUTION STATEMENT (of this Report)  Approved for public release; distribution unlimited		
17 DISTRIBUTION STATEMENT (of the abstract entered in Block 20, if different from Report)		
18 SUPPLEMENTARY NOTES		
19 KEY WORDS (Continue on reverse side if necessary and identify by block number) High Angle of Attack Missile Aerodynamics Side Forces Forces and Moments Induced Effects		
20 ABSTRACT (Continue on reverse side if necessary and identify by block number) Linear regression techniques are used to establish a quantitative description of side forces on bodies at high incidence. A data base is assembled concerning the key side force characteristics of maximum observed side force, angle of occurrence, and minimum angle of attack at which a side force is observed. This information is examined to determine the important trends and a predictive model for side force based on the crossflow analogy is		

DD FORM 1 JAN 73 1473

EDITION OF 1 NOV 65 IS OBSOLETE  
S N 0102-014-6601

UNCLASSIFIED

SECURITY CLASSIFICATION OF THIS PAGE (When Data Entered)



NSWC/WOL/TR 75-176

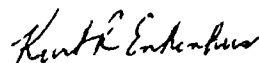
1 November 1975

INDUCED SIDE FORCES ON BODIES OF REVOLUTION AT HIGH  
ANGLE OF ATTACK

A large data base is collected from the open literature and private sources concerning key side force characteristics. Linear regression techniques are used to establish predictive equations which can be used by the designer.

The authors wish to thank K. D. Thomson, G. Brebner, B. Cheers, A. Maddox and J. Fidler who passed on the unpublished information used in the study.

This work was performed at the Naval Surface Weapons Center (NAVSURFWPNCEN/WOL) for the Naval Systems Command under task A320-0000/WF32-322-202.



KURT R. ENKENHUS  
By direction

## CONTENTS

	Page
INTRODUCTION . . . . .	6
PREDICTIVE MODEL BASED ON THE CROSSFLOW ANALOGY . . . . .	9
DATA BASE . . . . .	17
CREATION OF A REGRESSION MODEL . . . . .	31
COMPARISON OF REGRESSION AND CROSSFLOW MODEL . . . . .	34
CONCLUSIONS . . . . .	35

## TABLES

Table	Title	Page
1	Data Base . . . . .	18

## ILLUSTRATIONS

Figure	Title	Page
1	Variation of Leeward Flowfield With Change in Model Roll Angle . . . . .	7
2	$C_y$ as a Function of $\alpha$ at Several Different Roll Orientations . . . . .	8
3	$C_{Lrms}$ as a Function of $M$ for Cylinders in Crossflow . . . . .	12
4	$S$ as a Function of $M$ for Cylinders in Crossflow and $S$ as a Function of $M_C$ for Bodies at Incidence . . . . .	13
5	Crossflow Model Prediction of $C_{ym}$ . . . . .	15
6	Crossflow Model Prediction of $\alpha_m$ . . . . .	16
7	$C_{ym}$ as a Function of $M$ for All Points in the Data Base . . . . .	23
8	$C_{ym}$ as a Function of $M_C = M \sin \alpha_m$ for All Points in the Data Base for which $\alpha_m$ is Known . . . . .	24
9	$C_{ym}$ as a Function of $l_n$ for All Points in the Data Base . . . . .	25
10	$C_{ym}$ as a Function of $Re$ for All Data Points Having $M < .51$ . . . . .	26
11	$C_{ym}$ as a Function of $r_b$ for All Blunt Models ( $r_b > .005$ ) . . . . .	27

## ILLUSTRATIONS (Cont'd)

Figure	Title	Page
12	$\alpha_m$ as a Function of $\bar{I}_t$ for All Points in the Data Base where $\alpha_m$ is known and $C_{ym} > .75$ . Also Shown is Equation (8) . . . . .	28
13	$\alpha_m$ as a Function M for All Points in the Data Base where $\alpha_m$ is known and $C_{ym} > .75$ . . . . .	29
14	$\alpha_o$ as a Function of $\bar{I}_t$ for All Points in the Data Base Points where $\alpha_o$ is known and $C_{ym} > .75$ . Also Shown is the Crossflow Model Prediction, Equation (7) and the Linear Regression Model, Equation (8) . .	30

## LIST OF SYMBOLS

$C_L$	lift coefficient of cylinder in crossflow = $F_L/qDL$
$C_Y$	side force coefficient on a body at incidence - $F_Y/q\left(\frac{\pi D^2}{4}\right)$
$C_{ym}$	absolute value of maximum observed $C_Y$
$D$	local diameter
$\bar{D}$	average local diameter for entire body or portion of it
$D_b$	base diameter
$f$	frequency of vortex shedding
$F_L$	side force on cylinder in crossflow
$F_Y$	side force on body at incidence
$l$	length along body / $\bar{D}$
$l_b$	model afterbody length / $D_b$
$l_n$	nose length / $D_b$
$l_o$	virtual nose length / $D_b$
$l_s$	$x_s/\bar{D}$
$l_t$	model length / $D_b$
$\bar{I}_t$	$(\text{model length})^2 / \text{planar cross-sectional area} =$ model length / $\bar{D}$
$M$	Mach number
$M_{crit}$	critical Mach number
$M_c$	crossflow Mach number = $M \sin \alpha$
$q$	free stream dynamic pressure
$Re$	free stream Reynolds number based on diameter

$Re_c$	crossflow $Re = Re \sin \alpha$
$r_b$	nose tip radius $/D_b$
$S$	Strouhal number $= Df/U$
$t$	time
$t^*$	dimensionless time
$U$	free stream velocity
$x$	longitudinal distance along a test model measured from nose tip
$x_s$	$\Delta x$ between the shedding of successive vortices
$\alpha$	angle of attack
$\alpha_F$	lowest $\alpha$ at which a complete constant sign side force interval is present
$\alpha_O$	onset angle (minimum angle of attack at which a side force is observed)
$\alpha_m$	angle of attack at which maximum side force is observed

## INTRODUCTION

Bodies with pitch plane symmetry experience steady or quasi-steady side loads at high angles of attack in the subsonic-transonic range. These forces generally occur between 20 to 60 degrees incidence and can be traced to the formation of an asymmetric vortex pattern in the leeward flow field. The magnitude of the side force has been observed to exceed that of the normal force on short bodies ( $l_t < 4$ ).<sup>1</sup>

To date, side forces have been the subject of several studies,<sup>1-4</sup> which have determined that the magnitude of these loads decreases with increasing Mach number, decreasing nose fineness, and the introduction of bluntness. No conclusions have been offered concerning the influence of Reynolds number, and the addition of grit has been observed to increase these forces in some cases, and decrease it in others.

A quantitative description of side forces has not emerged, these loads being extremely sensitive to factors that are difficult to control, such as extremely small irregularities in the model geometry and seemingly insignificant changes in test conditions and/or procedures. Rolling an axis-symmetry model drastically alters the measured side force and the accompanying vortex pattern as shown in Figures 1 and 2. The pictures of Figure 1 are unpublished results obtained at NAVSURFWPNCEN while the data of Figure 2 is from reference 5. The cause of this change has been traced by some observers to irregularities in model construction on the order of

1. Keener, Earl R. and Chapman, G. T., "Onset of Aerodynamic Side Forces at Zero Sideslip on Symmetric Forebodies at High Angles of Attack," AIAA Paper 74-770, 1974.
2. Pick, G., "Investigation of Side Forces on Ogive-Cylinder Bodies at High Angles of Attack in the  $M = 0.5$  to  $1.1$  Range," AIAA Paper No. 71-570, Jun 1971.
3. Fleeman, E. L. and Nelson, R. C., "Aerodynamic Forces and Moments on a Slender Body with a Jet Plume for Angles of Attack up to 180 Degrees," AIAA Paper No. 74-110, 1974.
4. Clark, W. H., Peoples, J. R. and Briggs, M. M., "Occurrence and Inhibition of Large Yawing Moments During High Incidence Flight of Slender Missile Configurations," J. Spacecraft, 10, 8, 1973, pp. 510-519.
5. Wardlaw, A. B., Jr., "The Prediction of Normal Force, Pitching Moment and Yaw Force on Bodies of Revolution at Angles of Attack Up to 50 Degrees Using a Concentrated Vortex Flow-Field Model", NOLTR 73-209, Oct 1973.

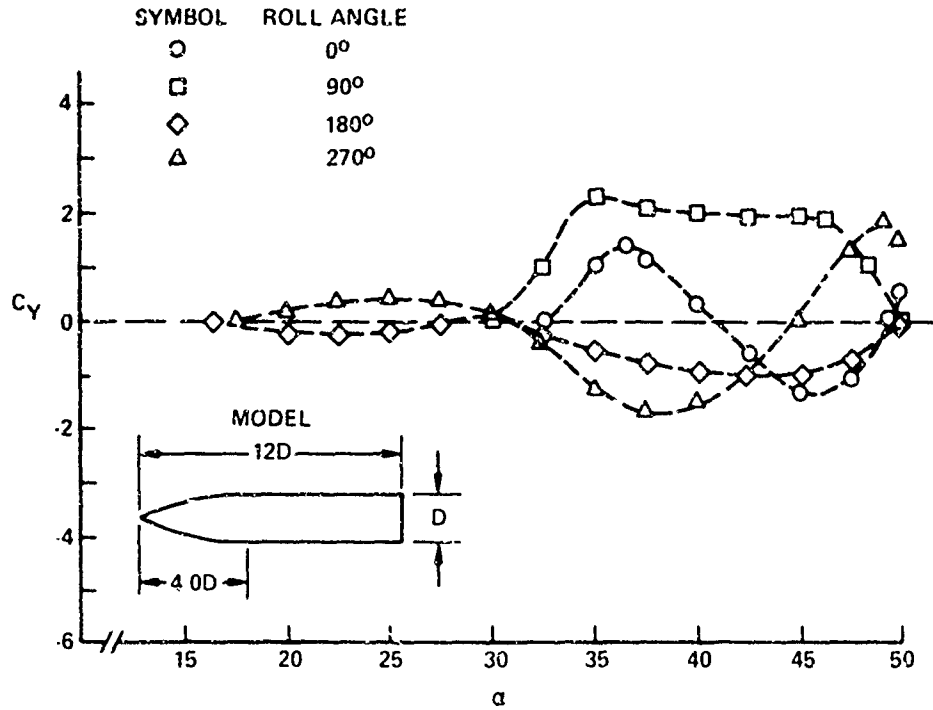


b)  $\phi = 90^\circ$   $M = 0.7$   $\alpha = 40^\circ$



a)  $\phi = 0^\circ$   $M = 0.7$   $\alpha = 40^\circ$

FIG 1 VARIATION OF THE LEEWARD FLOWFIELD WITH CHANGE IN THE MODEL ROLL ORIENTATION.

DATA TAKEN FROM REFERENCE 5. ( $M = 0.9$ )FIG. 2  $C_Y$  AS A FUNCTION OF  $\alpha$  AT SEVERAL DIFFERENT ROLL ORIENTATIONS.

machining tolerance;<sup>6</sup> however, the fact that side force measurements taken at roll angles differing by 180 degrees are not necessarily mirror images of one another (see Figure 2) indicates that other factors are important. In particular it raises the questions as to whether side force magnitude is facility dependent.

The definition of the high angle of attack flowfield is further complicated by wake instabilities which have been observed to be interspersed with the steady asymmetric mode.<sup>7</sup> Although the steady mode appears to be the dominant one, a completely steady asymmetric flow field and aerodynamic load model is an idealization of the situation. The results of reference 6, which at present stand alone, indicate a predominant unsteady mode at angles of attack as low as 10 degrees.

In the current report a quantitative description of key side force characteristics is developed by applying linear regression techniques to a collected data base. The data base is constructed from information available in the open literature and from private sources concerning the key features of maximum observable side force, angle of attack at which it occurs, and the lowest angle of attack at which a side force is observed. As a prelude to applying linear regression methods it is necessary to postulate a set of independent variables that is thought to influence each of these quantities. This could be approached from the dimension analysis point of view; however, this produces too many possible independent variables. Instead, an approximate model based on the crossflow analogy will be constructed to predict side force and its onset angle. The results of this analysis in conjunction with a detailed study of the data base will be used to postulate a set of independent variables related to each of the above quantities. The linear regression procedure will determine a least square fit for each of these quantities using only those independent variables which are statistically significant.

#### PREDICTIVE MODEL BASED ON THE CROSSFLOW ANALOGY

The crossflow analogy assumes that forces on a body at angle of attack are related to those acting on a cylinder in crossflow and has been extensively applied to the prediction of normal force. In its simplest form the steady state cylinder drag corresponding to  $M_C$  and  $Re_C$  is used in computing this quantity.<sup>8,9</sup> A more accurate approach

6. Gowen, F. E. and Perkins, E. W., "Study of the Effects of Body Shape on the Vortex Wakes of Inclined Bodies at  $M=2$ ," RM A53117, 1953, NACA.
7. Thomson, K. D. and Morrison, D. F., "The Spacing, Position and Strength of Vortices in the Wake of Slender Cylindrical Bodies at Large Incidence," J. Fluid Mechanics, 50 4, 1971, pp. 751-783.
8. Allen, H. J., "Estimation of Forces and Moments on Inclined Bodies of Revolution of High Fineness Ratio," NACA RM A9126, 1949.
9. Jorgensen, L. H., "Prediction of Static Aerodynamic Characteristics for Space-Shuttle-Like and Other Bodies at Angles of Attack from  $0^\circ$  to  $180^\circ$ ," NASA TN D-6996, Jan 1973.

assumes that the crossflow plane is swept down the length of the incident body at the uniform rate  $U \cos \alpha$ . Distance along the body is related to time in the case of a cylinder by:

$$t = x/(U \cos \alpha) \quad (1)$$

At any point along the model length the steady state drag value is replaced by that of an impulsively started cylinder at its equivalent time  $t$ . This approach was originally suggested by Kelly<sup>10</sup> and has since been used in various forms by others.

In considering a predictive model for side force, it is necessary to use the second approach since the lift on a cylinder is unsteady while  $C_y$  on a body at incidence is steady. Hence:

$$F_Y = \int_0^L F_L(t=x/U \cos \alpha, M_C, Re_C) dx \quad (2)$$

Ideally  $F_L$  would be based on data for an impulsively started, expanding cylinder. Unfortunately, this type of information is not available so time independent root mean square values are used.

Substitution of the unsteady lift of a cylinder in crossflow into the right hand side of Equation (2) results in a force distribution which varies periodically from positive to negative along the length of the body. Since the frequency for the shedding of consecutive vortices on a cylinder is:

$$f = 2US/D \quad (3)$$

the distance along the body sustaining a force of constant sign is:

$$x_s = \bar{D}/(2 S \tan \alpha) \text{ or } l_s = 1/(2 S \tan \alpha) \quad (4)$$

Hence, the maximum unbalanced side force is obtained by integrating Equation (2) between the limits  $C$  and  $C + x_s$  where  $C$  marks the distance in  $x$  at which the side force changes sign. Such an interval containing a force of constant sign will be referred to as a cell. In terms of yaw and lift force coefficients Equation (2) becomes:

10. Kelly, H. R., "The Estimation of Normal Force, Drag, and Pitching-Moment Coefficients for Blunt Based Bodies of Revolution at Large Angle of Attack," Journal of Aeronautical Sciences, Vol. 21, No. 8, pp. 549-555.

$$C_{ym} \sim \frac{4\bar{D} \sin^2 \alpha}{\pi D^2} \int_C^{C + \bar{D}/(2 S \tan \alpha)} C_L dx \quad (5)$$

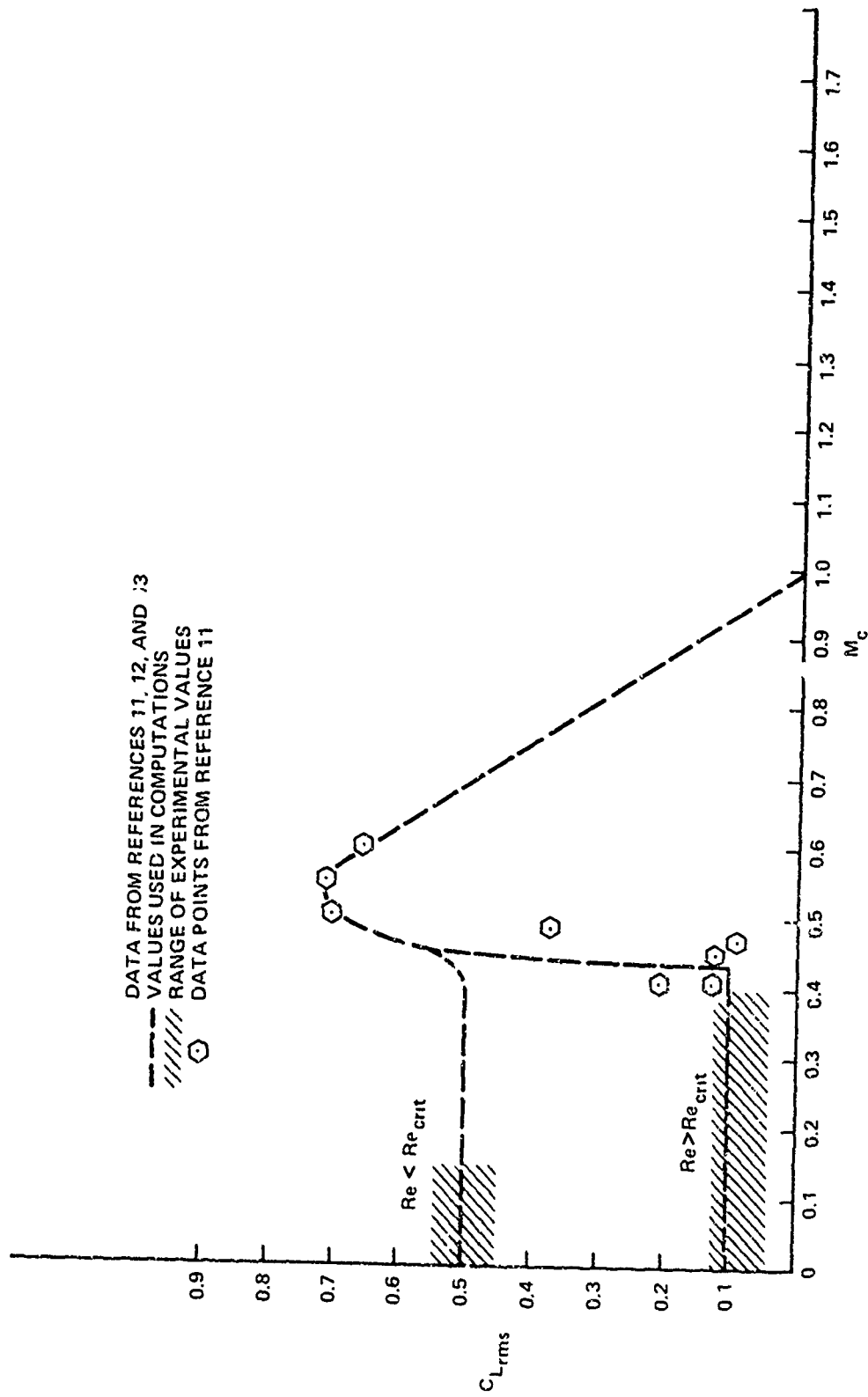
Here  $\bar{D}$  represents an average value for  $D$  over the length of the shedding interval.  $C_L$  is generally expressed by its root mean square value and assuming that this measurement is generated either by sine or square wave results in:

$$C_{ym} \sim \frac{.3 \sin(2\alpha) C_{L_{rms}}}{S} \left( \frac{\bar{D}}{D} \right)^2 \quad (6)$$

The extent of the available experimental values for  $C_L$  and  $S$  are given in Figures 3 and 4 respectively and have been taken from references 11 through 14. The shaded area represents the range in measured values for given test conditions. Although the incompressible case is well documented, very little information is available in the transonic or supersonic regime. Transonic measurements, taken at supercritical Reynolds numbers, indicate that as the Mach number is increased past the critical point,  $C_L$  changes noticeably assuming a new value that is similar to that for the laminar case.<sup>11</sup> This same type of behavior is characteristic of the cylinder drag. For supersonic conditions no direct measurements are available; however, Schlieren photographs show a symmetric wake structure.<sup>14</sup> Based on this evidence it is likely that  $C_L = 0$  under these conditions. In Figure 4, the measurements of reference 7 for  $S$  on a body at incidence with laminar boundary layer are shown. These agree well with those taken on a cylinder in crossflow.

The preceding model does not provide a prediction of onset angle. To develop such an expression the sequence of events accompanying the formation of the flow field about an impulsively started body is

11. Jones, G. W., Cincotta, J. J., and Walker, R. W., "Aerodynamic Forces on a Stationary and Oscillating Circular Cylinder at High Reynolds Number," Oct 1968, NASA TR R-300.
12. Bearman, P. W., "On Vortex Shedding From a Circular Cylinder in the Critical Reynolds Number Regime," J. Fluid Mech., Vol. 37, Part 3, pp. 577-585, 1969.
13. Richter, Andreas, Flow Force on Rigid Circular Cylinder Between Parallel Walls, (in German), PH.D. Dissertation, Karlsruhe, 1973.
14. Gowen, F. E. and Perkins, E. W., "Drag of Circular Cylinders for a Wide Range of Reynolds Numbers and Mach Numbers," NACA RM A52C20, Jun 1952.

FIG. 3  $C_{Lrms}$  AS A FUNCTION OF  $M_c$  FOR CYLINDERS IN CROSSFLOW.

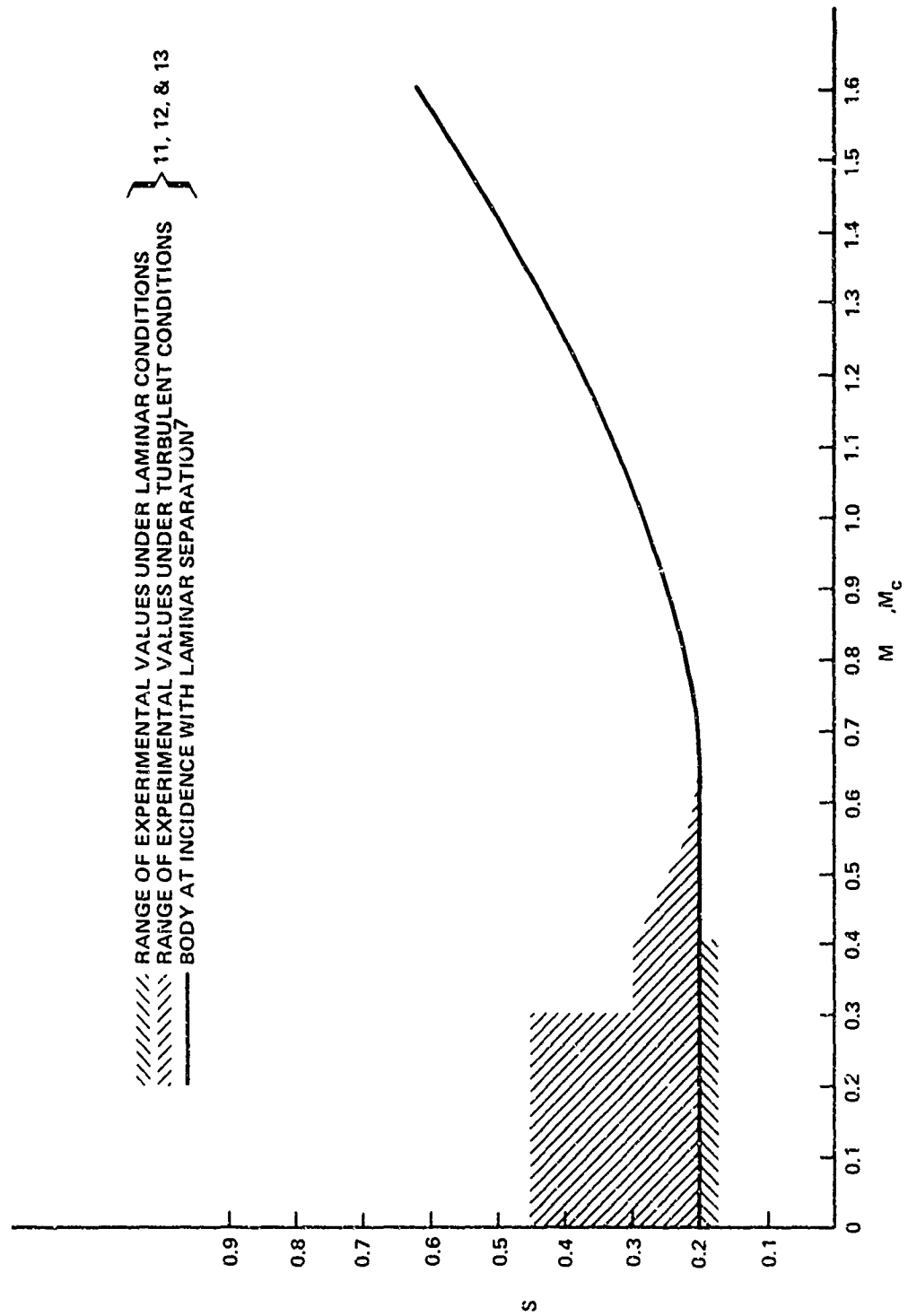


FIG. 4  $S$  AS A FUNCTION OF  $M$  FOR CYLINDERS IN CROSSFLOW AND  $S$  AS A FUNCTION OF  $M_c$  FOR BODIES AT INCIDENCE.

considered. Sarpkaya's data<sup>15</sup> taken in incompressible flow over the Reynolds number range  $1.5 \times 10^4$  to  $1.2 \times 10^5$  indicates that the flowfield remains symmetric for an initial period  $t_s^* = Ut/D = 4$ . Generalizing to a body at incidence and using  $\bar{D}$  in place of  $D$  to account for the changing body diameter near the nose:

$$t_s^* = x(\tan \alpha_o)/\bar{D} = 4$$

and

$$\alpha_o = \tan^{-1} (4/\bar{l}_t) \quad (7)$$

Equation (7) does not indicate the effect of Mach number on  $\alpha_o$ . Based on slender body crossflow theory it might be expected that this effect would not be of great importance since  $\alpha_o$  is often relatively small.

To produce a side force estimate continuous in  $\alpha$ , it is necessary to define  $\alpha_F$  as the lowest angle of attack at which a complete cell exists on the body. To determine  $\alpha_F$ ,  $l_t - l_s$  is used in place of  $x$  in Equation (7):

$$\alpha_F = \tan^{-1} \left\{ \frac{4}{\bar{l}_t} + \frac{1}{2S\bar{l}_t} \right\} \quad (8)$$

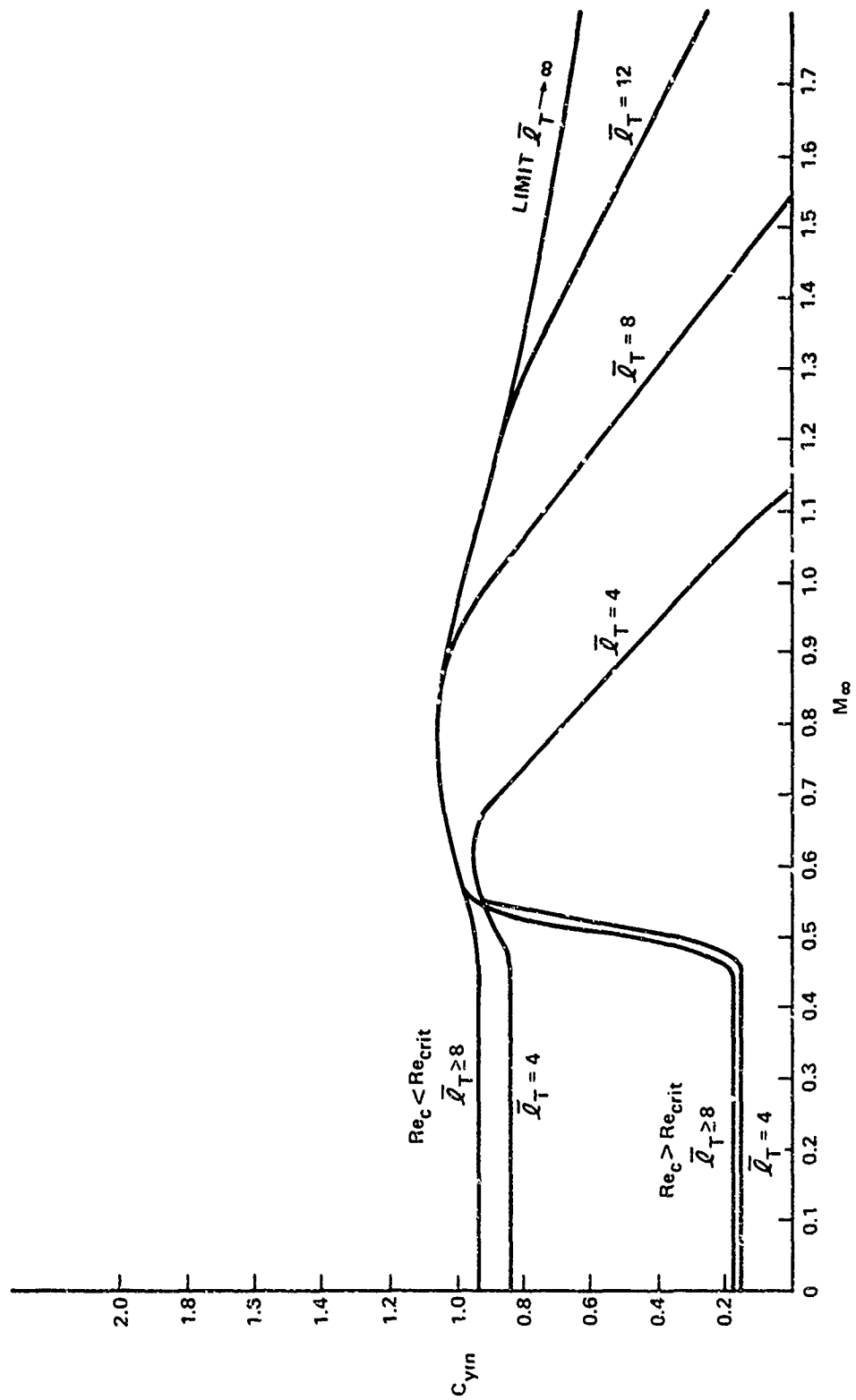
If  $\alpha$  is between  $\alpha_o$  and  $\alpha_F$ , only the following fraction of the cell is present:

$$\frac{l}{l_s} = 2S \left[ \bar{l}_t \tan \alpha - 4 \right]$$

If a sine force distribution is assumed along the length of the body at incidence, the value of  $C_{ym}$  calculated in Equation (6) must be multiplied by the correction factor  $F = (1/2 - 1/2 \cos [\pi l/l_s])$  in the angle of attack range  $\alpha_o$  to  $\alpha_F$ .

The predictions of the crossflow model are summarized in Figures 5 and 6. In these graphs it has been assumed that the maximum incidence at which a steady side force occurs is 60 degrees. The value of  $C_L$  used is indicated by the dotted line in Figure 4 and  $S$  is taken as  $.17 \sim .2$ . The calculated curves in Figures 5 and 6 reflect the fact

15. Sarpkaya, T., "Separated Flow About Lifting Bodies and Impulsive Flow About Cylinders," IAA Journal, Vol. 4, No. 3, 1966, pp. 414-420.

FIG. 5 CROSSFLOW MODEL PREDICTION OF  $C_{ym}$

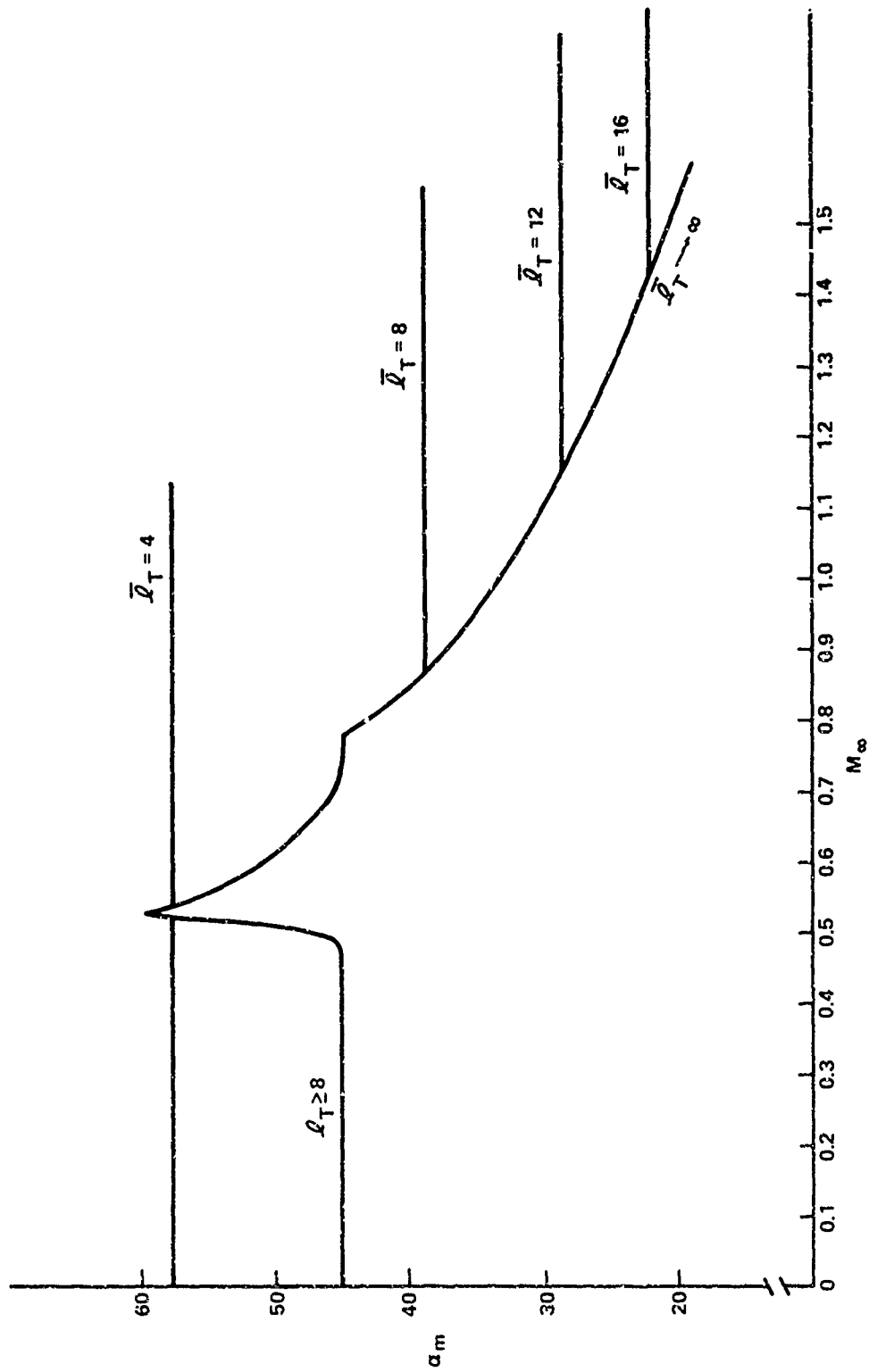


FIG. 6 CROSSFLOW MODEL PREDICTION OF  $\alpha_m$

that the maximum side loads occur at  $\alpha = 45^\circ$  for  $M < .46$  as suggested by Equation (6). At higher Mach numbers, variations in  $C_L$  dominate over the angular dependence of this equation and  $C_{ym}$  is located at the angle of attack at which  $M_C = .55$  and  $C_L$  has its peak value. In the incidence range  $\alpha_0$  to  $\alpha_F$ ,  $F$  decreases rapidly with decreasing  $\alpha$  and the peak side force occurs at  $\alpha_F$ . For  $\bar{l}_t < 8$ ,  $\alpha_F$  is greater than  $45^\circ$  which explains the unique characteristics of the  $\bar{l}_t = 4$  curve.

The crossflow model indicates that  $C_{ym}$  is a function of  $M$  and  $Re$  for  $M_C < M_{crit}$ . The model length,  $\bar{l}_t$ , is only important at high Mach numbers and on very short models, while nose geometry is significant only for models without afterbodies. In this case  $C_{ym}$  decreases with decreasing  $\bar{l}_n$  since  $\bar{D}$  becomes smaller under these conditions. The variable  $\alpha_m$  is dependent on  $M$  and  $\bar{l}_t$  while  $\alpha_0$  is a function of  $\bar{l}_t$  only.

#### DATA BASE

The collected data base is given in Table 1 and is directly read from references 1 through 3, 5, and 16 through 24. The tabulated quantities  $C_{ym}$ ,  $\alpha_m$ , and  $\alpha_0$  represent the absolute value of the maximum side force, the angle of attack at which it occurs, and the lowest angle at which a side force is measured, respectively.

16. Smith, L. H. and Nunn R. H., "Aerodynamic Characteristics of an Axisymmetric Body Undergoing a Uniform Pitching Motion," Naval Postgraduate School, NPS-59Nn75021, Feb 1975.
17. Coe, P. L., Jr. and Chambers, J. R., "Asymmetric Lateral-Directional Characteristics of Pointed Bodies of Revolution at High Angles of Attack," NASA TN D-7095, Nov 1972.
18. Jorgensen, L. H. and Nelson, E. R., "Experimental Aerodynamics Characteristics for a Cylindrical Body of Revolution with Various Noses at Angles of Attack from 0 to  $58^\circ$  and Mach Numbers from .6 to 2.0," NASA TMX-3128, Dec 1974.
19. Jorgensen, L. H. and Nelson, E. R., "Experimental Aerodynamic Characteristics for Bodies of Elliptic Cross Section at Angles of Attack from 0 to  $58^\circ$  and Mach Numbers from .6 to 2.0," NASA TMX-3129, Feb 1975.
20. Daniels, P., "Minimization of Lock-in Roll Moment on Missiles via Slots," NSWC/DL Technical Report TR-3250, Jan 1975.
21. Fellows, K. A., "Tests on an Ogive Cylinder up to Very High Incidences at Transonic Speeds," Aircraft Research Association Limited, Bedford, Great Britain, Model Test Note M.61/1.
22. Brown, R. C., "On the Asymmetrical Aerodynamic Forces of Slender Bodies of Revolution," Proceedings of BOWACA Meeting, 1965.
23. "Unpublished Tests on Cone-Cylinder at Incidences up to  $70^\circ$ ," provided by K. D. Thomson, Australian Research Laboratory, Nov 1971.
24. Fidler, J., Unpublished Data Taken in NSRDC Transonic Tunnel, Private Communication, Mar 1973.

Table 1

No.	ECBY TYPE	M	$\alpha_D \times 10^{-5}$	$i_n$	BCDY GEOMETRY			$C_{ym}$	$C'_{ym}$	$\alpha_{ym}$	$\alpha'_{ym}$	$\alpha_o$	REFERENCE
					$r_b$	$i_o$	$i_b$						
1	1	.25	8.00	3.50	0.00	3.50	-0.00	1.17	-0.00	45.00	-0.00	25.00	1
2	-0	.25	8.00	3.50	0.00	3.50	-0.00	2.45	-0.00	55.00	-0.00	35.00	1
3	-0	.25	8.00	5.00	0.00	5.00	-0.00	2.46	-0.00	40.00	-0.00	25.00	1
4	2	.25	8.00	3.50	0.00	3.50	-0.00	3.11	-0.00	50.00	-0.00	25.00	1
5	-0	.25	20.00	3.50	0.00	3.50	-0.00	.61	-0.00	60.00	-0.00	32.00	1
6	-0	.25	28.00	3.50	0.00	3.50	-0.00	1.41	-0.00	55.00	65.00	30.00	1
7	-0	.25	8.00	3.50	0.00	3.50	-0.00	2.89	-0.00	55.00	-0.00	32.00	1
8	-0	.25	8.00	3.50	0.00	3.50	3.50	1.00	1.00	45.00	60.00	30.00	1
9	-0	.25	8.00	3.50	0.00	3.50	3.50	.89	.89	45.00	60.00	25.00	1
10	-0	.25	28.00	3.50	0.00	3.50	3.50	3.11	3.11	40.00	50.00	25.00	1
11	-0	.25	20.00	3.50	0.00	3.50	3.50	2.89	-0.00	35.00	-0.00	25.00	1
12	-0	.25	8.00	3.50	0.00	3.50	-0.00	2.89	-0.00	60.00	-0.00	35.00	1
13	-0	.25	8.00	3.50	0.00	3.50	-0.00	2.67	-0.00	55.00	-0.00	37.00	1
14	-0	.25	8.00	3.50	0.00	3.50	-0.00	3.00	-0.00	55.00	-0.00	35.00	1
15	-0	.25	8.00	3.50	0.00	3.50	-0.00	2.56	-0.00	50.00	-0.00	35.00	1
16	-0	.25	8.00	3.50	0.00	3.50	-0.00	2.00	-0.00	50.00	-0.00	40.00	1
17	-0	.25	8.00	3.50	0.00	3.50	0.00	2.85	-0.00	55.00	-0.00	40.00	1
18	-0	.25	8.00	3.50	0.00	3.50	0.00	1.65	-0.00	65.00	-0.00	35.00	1
19	-0	.25	8.00	3.42	.02	3.50	0.00	.72	-0.00	50.00	-0.00	40.00	1
20	-0	.25	8.00	3.20	.08	3.50	0.00	.78	-0.00	55.00	-0.00	45.00	1
21	-0	.25	8.00	3.35	.04	3.50	0.00	.39	-0.00	45.00	-0.00	35.00	1
22	-0	.25	8.00	3.50	0.00	3.50	0.00	2.44	-0.00	55.00	-0.00	35.00	1
23	-0	.25	8.00	3.50	0.00	3.50	0.00	.42	-0.00	55.00	-0.00	35.00	1
24	-0	.25	8.00	3.50	0.00	3.50	0.00	0.00	-0.00	-0.00	-0.00	-0.00	1
25	-0	.25	8.00	5.00	0.00	5.00	0.00	2.34	-0.00	-0.00	-0.00	-0.00	1
26	-0	.25	8.00	5.00	0.00	5.00	0.00	2.29	-0.00	-0.00	-0.00	-0.00	1
27	-0	.25	8.00	5.00	0.00	5.00	0.00	2.14	-0.00	-0.00	-0.00	-0.00	1
28	1	.25	8.00	3.50	0.00	3.50	0.00	1.26	-0.00	-0.00	-0.00	-0.00	1
29	1	.25	8.00	3.50	0.00	3.50	0.00	1.02	-0.00	-0.00	-0.00	-0.00	1
30	1	.25	8.00	3.50	0.00	3.50	0.00	.77	-0.00	-0.00	-0.00	-0.00	1
31	2	.25	8.00	3.50	0.00	3.50	0.00	2.16	-0.00	-0.00	-0.00	-0.00	1
32	2	.25	8.00	3.50	0.00	3.50	0.00	.77	-0.00	-0.00	-0.00	-0.00	1
33	2	.25	8.00	3.50	0.00	3.50	0.00	.54	-0.00	-0.00	-0.00	-0.00	1
34	-0	.25	8.00	3.50	0.00	3.50	0.00	.98	-0.00	-0.00	-0.00	-0.00	1
35	-0	.25	8.00	3.50	0.00	3.50	0.00	1.99	-0.00	-0.00	-0.00	-0.00	1
36	-0	.25	8.00	3.50	0.00	3.50	0.00	2.00	-0.00	-0.00	-0.00	-0.00	1
37	-0	.25	8.00	3.50	0.00	3.50	0.00	1.16	-0.00	40.00	-0.00	-0.00	3
38	-0	.25	2.30	-0.00	-0.00	-0.00	-0.00	.94	-0.00	35.00	-0.00	-0.00	3
39	-0	.25	5.00	3.00	0.00	3.00	12.00	3.70	-0.00	45.00	-0.00	17.00	14
40	-0	.25	1.40	3.00	0.00	3.00	12.00	2.49	-0.00	50.00	-0.00	17.00	16
41	-0	.25	1.40	3.00	0.00	3.00	12.00	2.44	-0.00	50.00	-0.00	17.00	16
42	-0	.25	3.50	3.50	0.00	3.50	0.00	3.10	-0.00	55.00	-0.00	30.00	17
43	-0	.25	2.10	3.50	0.00	3.50	0.00	3.10	-0.00	55.00	-0.00	30.00	17
44	-0	.25	1.50	3.50	0.00	3.50	0.00	2.86	-0.00	55.00	-0.00	30.00	17
45	-0	.25	2.10	3.50	0.00	3.50	3.50	4.00	-0.00	48.00	-0.00	30.00	17
46	1	.25	2.10	3.50	0.00	3.50	0.00	1.40	1.20	40.00	55.00	20.00	17
47	1	.25	3.50	3.50	0.00	3.50	0.00	1.20	1.20	40.00	55.00	20.00	17
48	2	.25	3.50	3.50	0.00	3.50	0.00	.20	-0.00	-0.00	-0.00	15.00	17
49	-0	.25	6.50	3.00	0.00	3.00	7.00	.30	-0.00	57.50	0.00	57.50	18,19
50	-0	.25	6.50	3.50	0.00	3.50	7.00	2.50	-0.00	51.00	-0.00	26.00	18,19
51	-0	.25	6.50	5.00	0.00	5.00	7.00	1.90	-0.00	40.50	-0.00	28.00	18,19
52	-0	.25	6.50	2.50	0.00	2.50	7.00	.40	-0.00	51.00	-0.00	46.00	18,19
53	-0	.25	6.50	3.00	0.00	3.00	7.00	.30	-0.00	30.00	-0.00	30.00	18,19
54	-0	.25	6.50	3.50	0.00	3.50	7.00	1.30	-0.00	26.00	-0.00	26.00	18,19
55	-0	.25	6.50	5.00	0.00	5.00	7.00	2.00	-0.00	41.00	-0.00	26.00	18,19
56	-0	.25	6.50	2.50	0.00	2.50	7.00	.50	-0.00	57.50	-0.00	48.00	18,19
57	-0	1.20	3.80	3.00	0.00	3.00	7.00	.20	-0.00	-0.00	-0.00	-0.00	18,19
58	-0	1.20	3.80	3.50	0.00	3.50	7.00	.70	-0.00	38.00	-0.00	30.00	18,19
59	-0	1.20	3.50	5.00	0.00	5.00	7.00	.40	-0.00	28.00	-0.00	20.00	18,19

\* BCDY type is: tangent of  $\alpha = 0$ , cone = 1, paraboloid = 2

Table 1 (Cont'd)

NO.	BODY TYPE	M	R <sub>0</sub>	X	0-5	BODY GEOMETRY	b <sub>0</sub>	b <sub>1</sub>	C <sub>ym</sub>	C <sub>ym</sub>	$\alpha_m'$	$\alpha_m$	REFERENCE
40	-6	1.20	3.80	2.50	2.50	0.00	7.00	7.00	.40	-0.00	-0.00	32.00	18,19
41	-0	1.50	3.80	3.00	3.00	0.00	7.00	7.00	0.00	-0.00	-0.00	-0.00	18,19
42	-6	1.50	3.80	3.50	3.50	0.00	7.00	7.00	0.00	-0.00	-0.00	-0.00	18,19
43	-0	1.50	3.80	5.00	5.00	0.00	7.00	7.00	0.00	-0.00	-0.00	-0.00	18,19
44	-0	1.50	3.80	2.50	2.50	0.00	7.00	7.00	0.00	-0.00	-0.00	-0.00	18,19
45	-0	2.00	3.80	3.00	3.00	0.00	7.00	7.00	0.00	-0.00	-0.00	-0.00	18,19
46	-0	2.00	3.80	3.50	3.50	0.00	7.00	7.00	0.00	-0.00	-0.00	-0.00	18,19
47	-0	2.00	3.80	5.00	5.00	0.00	7.00	7.00	0.00	-0.00	-0.00	-0.00	18,19
48	-0	2.00	3.80	2.50	2.50	0.00	7.00	7.00	0.00	-0.00	-0.00	-0.00	18,19
49	-0	.60	6.50	3.00	3.00	.18	3.50	7.00	1.40	-0.00	-0.00	51.00	18,19
70	-0	.90	6.50	3.00	3.00	.18	3.50	7.00	.70	-0.00	-0.00	30.00	18,19
71	-0	1.20	3.80	3.00	3.00	.18	3.50	7.00	.20	-0.00	-0.00	24.00	18,19
72	-0	1.50	3.80	3.00	3.00	.18	3.50	7.00	0.00	-0.00	-0.00	-0.00	18,19
73	-0	2.00	3.80	3.00	3.00	.18	3.50	7.00	0.00	-0.00	-0.00	-0.00	18,19
74	-0	.14	4.30	2.95	.03	3.00	6.00	6.00	1.83	-0.00	-0.00	63.00	20
75	-0	.60	2.20	3.00	0.00	3.00	3.00	7.00	.70	-0.00	-0.00	54.00	18
76	-0	.60	4.30	3.00	0.00	3.00	7.00	7.00	1.80	-0.00	-0.00	57.50	18
77	-0	.50	2.20	3.00	0.00	3.00	3.00	7.00	.60	-0.00	-0.00	57.50	18
78	-0	.90	4.30	3.00	0.00	3.00	7.00	7.00	.60	-0.00	-0.00	57.50	18
79	-0	.60	2.20	5.00	0.00	5.00	7.00	7.00	2.20	-0.00	-0.00	40.00	18
80	-0	.60	4.30	5.00	0.00	5.00	7.00	7.00	3.60	-0.00	-0.00	36.00	18
91	-0	.50	2.20	5.00	0.00	5.00	7.00	7.00	2.50	-0.00	-0.00	30.00	18
82	-0	.70	4.30	5.00	0.00	5.00	7.00	7.00	2.40	-0.00	-0.00	32.00	18
83	-0	.70	11.10	1.50	0.00	1.50	9.50	9.50	.40	-0.00	-0.00	68.00	21
84	-0	.70	9.40	1.50	0.00	1.50	9.50	9.50	.40	-0.00	-0.00	68.00	21
85	-0	.70	7.40	1.50	0.00	1.50	9.50	9.50	.65	-0.00	-0.00	68.00	21
86	-0	.85	9.40	1.50	0.00	1.50	9.50	9.50	.60	-0.00	-0.00	23.00	21
87	-0	.95	9.40	1.50	0.00	1.50	9.50	9.50	.60	-0.00	-0.00	42.00	21
88	-0	1.05	9.40	1.50	0.00	1.50	9.50	9.50	.40	-0.00	-0.00	44.00	21
89	-0	1.15	9.40	1.50	0.00	1.50	9.50	9.50	.24	-0.00	-0.00	40.00	21
90	-0	1.30	9.40	1.50	0.00	1.50	9.50	9.50	.10	-0.00	-0.00	33.00	21
91	-0	.50	3.40	1.87	.00	1.87	8.17	8.17	3.29	-0.00	-0.00	50.00	22
92	-0	.70	3.40	2.75	.10	3.00	8.00	8.00	1.09	-0.00	-0.00	37.00	22
93	-0	.70	3.40	2.75	.10	3.00	8.00	8.00	1.10	-0.00	-0.00	37.00	22
94	-0	1.10	4.20	3.03	.03	4.00	8.00	8.00	1.13	-0.00	-0.00	34.00	22
95	-0	1.10	4.20	3.03	.03	4.00	8.00	8.00	1.18	-0.00	-0.00	35.00	22
96	-0	1.10	4.20	3.03	.03	4.00	8.00	8.00	.86	-0.00	-0.00	36.00	22
97	-0	.50	2.60	2.95	.03	3.00	8.00	8.00	1.42	-0.00	-0.00	36.00	22
98	-0	.60	2.40	2.95	.03	3.00	8.00	8.00	1.68	-0.00	-0.00	40.00	22
99	-0	.70	3.40	2.95	.03	3.00	8.00	8.00	.88	-0.00	-0.00	40.00	22
100	-0	.80	3.70	2.95	.03	3.00	8.00	8.00	.46	-0.00	-0.00	47.00	22
101	-0	.90	3.90	2.95	.02	3.00	8.00	8.00	.23	-0.00	-0.00	36.00	22
102	-0	1.10	4.20	2.95	.03	3.00	8.00	8.00	.21	-0.00	-0.00	33.00	22
103	-0	.50	2.00	1.98	.03	2.00	8.00	8.00	.50	-0.00	-0.00	40.00	22
104	-0	.70	3.40	1.98	.03	2.00	8.00	8.00	.70	-0.00	-0.00	40.00	22
105	-0	.80	3.70	1.98	.03	2.00	8.00	8.00	.32	-0.00	-0.00	37.00	22
106	-0	.90	3.90	1.98	.03	2.00	8.00	8.00	.32	-0.00	-0.00	37.00	22
107	-0	1.10	4.20	1.98	.03	2.00	8.00	8.00	.05	-0.00	-0.00	37.00	22
108	-0	.50	2.00	2.75	.10	3.00	8.00	8.00	1.32	-0.00	-0.00	36.00	22
109	-0	.60	2.40	2.75	.10	3.00	8.00	8.00	.91	-0.00	-0.00	33.00	22
110	-0	.70	3.40	2.75	.10	3.00	8.00	8.00	1.18	-0.00	-0.00	37.00	22
111	-0	.80	3.70	2.75	.10	3.00	8.00	8.00	.73	-0.00	-0.00	39.00	22
112	-0	1.10	4.20	2.75	.10	3.00	8.00	8.00	.37	-0.00	-0.00	31.00	22
113	-0	.50	2.40	3.05	.25	4.00	8.00	8.00	1.05	-0.00	-0.00	35.00	22
114	-0	.70	3.40	3.05	.25	4.00	8.00	8.00	.98	-0.00	-0.00	35.00	22
115	-0	.80	3.70	3.05	.25	4.00	8.00	8.00	.84	-0.00	-0.00	36.00	22
116	-0	.90	3.90	3.05	.25	4.00	8.00	8.00	1.19	-0.00	-0.00	36.00	22
117	-0	1.10	4.20	3.05	.25	4.00	8.00	8.00	.60	-0.00	-0.00	31.00	22
118	-0	.60	2.40	4.00	0.00	4.00	8.00	8.00	1.68	-0.00	-0.00	40.00	22
119	-0	.60	2.60	3.60	.10	4.00	8.00	8.00	.14	-0.00	-0.00	37.00	22

Table 1 (Cont'd)

No.	BCD TYPE	N	REP.X.0.5	$I_n$	BCDY GEOMETRY	$r_b$	$l_c$	$l_b$	$C_{ym}$	$C'_{ym}$	$\alpha'_{nm}$	$\alpha'_n$	$\alpha_n$	REFERENCE
120	-0	.60	2.40	3.05	.25	4.00	8.00	8.00	.98	-0.00	35.00	-0.00	20.00	2
121	-0	.50	2.00	4.00	0.00	4.00	8.00	8.00	4.00	-0.00	-0.00	-0.00	-0.00	2
122	-0	.40	2.60	4.00	0.00	4.00	8.00	8.00	2.27	-0.00	-0.00	-0.00	-0.00	2
123	-0	.70	3.40	4.00	0.00	4.00	8.00	8.00	1.89	-0.00	-0.00	-0.00	-0.00	2
124	-0	.80	3.70	4.00	0.00	4.00	8.00	8.00	1.46	-0.00	-0.00	-0.00	-0.00	2
125	-0	.50	3.50	4.00	0.00	4.00	8.00	8.00	.87	-0.00	-0.00	-0.00	-0.00	2
126	-0	1.10	4.20	4.00	0.00	4.00	8.00	8.00	1.32	-0.00	-0.00	-0.00	-0.00	2
127	-0	.50	2.00	3.93	.03	4.00	8.00	8.00	1.39	-0.00	-0.00	-0.00	-0.00	2
128	-0	.50	2.00	3.93	.03	4.00	8.00	8.00	1.91	-0.00	-0.00	-0.00	-0.00	2
129	-0	.70	3.40	3.93	.03	4.00	8.00	8.00	1.63	-0.00	-0.00	-0.00	-0.00	2
130	-0	.50	3.70	3.93	.03	4.00	8.00	8.00	1.30	-0.00	-0.00	-0.00	-0.00	2
131	-0	.50	3.00	3.93	.03	4.00	8.00	8.00	1.00	-0.00	-0.00	-0.00	-0.00	2
132	-0	1.10	4.20	3.93	.03	4.00	8.00	8.00	1.25	-0.00	-0.00	-0.00	-0.00	2
133	-0	.50	2.00	3.85	.05	4.00	8.00	8.00	.82	-0.00	-0.00	-0.00	-0.00	2
134	-0	.50	2.00	3.85	.05	4.00	8.00	8.00	.93	-0.00	-0.00	-0.00	-0.00	2
135	-0	.50	3.70	3.85	.05	4.00	8.00	8.00	.79	-0.00	-0.00	-0.00	-0.00	2
136	-0	.50	3.90	3.85	.05	4.00	8.00	8.00	.77	-0.00	-0.00	-0.00	-0.00	2
137	-0	1.10	4.20	3.85	.05	4.00	8.00	8.00	.80	-0.00	-0.00	-0.00	-0.00	2
138	-0	.50	2.00	3.68	.10	4.00	8.00	8.00	.43	-0.00	-0.00	-0.00	-0.00	2
139	-0	.50	2.60	3.68	.10	4.00	8.00	8.00	.49	-0.00	-0.00	-0.00	-0.00	2
140	-0	.50	3.70	3.68	.10	4.00	8.00	8.00	.64	-0.00	-0.00	-0.00	-0.00	2
141	-0	.50	3.50	3.68	.10	4.00	8.00	8.00	.11	-0.00	-0.00	-0.00	-0.00	2
142	-0	1.10	4.20	3.68	.10	4.00	8.00	8.00	.25	-0.00	-0.00	-0.00	-0.00	2
143	-0	.50	2.00	3.05	.25	4.00	8.00	8.00	.66	-0.00	-0.00	-0.00	-0.00	2
144	-0	.50	2.40	3.05	.25	4.00	8.00	8.00	1.16	-0.00	-0.00	-0.00	-0.00	2
145	-0	.70	3.50	3.05	.25	4.00	8.00	8.00	1.07	-0.00	-0.00	-0.00	-0.00	2
146	-0	.50	3.70	3.05	.25	4.00	8.00	8.00	.86	-0.00	-0.00	-0.00	-0.00	2
147	-0	1.10	4.20	3.05	.25	4.00	8.00	8.00	1.20	-0.00	-0.00	-0.00	-0.00	2
148	-0	.50	2.00	4.00	0.00	4.00	8.00	8.00	.50	-0.00	-0.00	-0.00	-0.00	2
149	-0	.50	2.60	4.00	0.00	4.00	8.00	8.00	3.07	-0.00	-0.00	-0.00	-0.00	2
150	-0	.50	3.40	4.00	0.00	4.00	8.00	8.00	3.00	-0.00	-0.00	-0.00	-0.00	2
151	-0	.70	3.60	4.00	0.00	4.00	8.00	8.00	2.63	-0.00	-0.00	-0.00	-0.00	2
152	-0	.50	3.00	4.00	0.00	4.00	8.00	8.00	.80	-0.00	-0.00	-0.00	-0.00	2
153	-0	1.10	4.20	4.00	0.00	4.00	8.00	8.00	1.32	-0.00	-0.00	-0.00	-0.00	2
154	-0	.50	2.00	3.00	0.00	3.00	8.00	8.00	1.11	-0.00	-0.00	-0.00	-0.00	2
155	-0	.50	2.40	3.00	0.00	3.00	8.00	8.00	.71	-0.00	-0.00	-0.00	-0.00	2
156	-0	.70	3.40	3.00	0.00	3.00	8.00	8.00	.71	-0.00	-0.00	-0.00	-0.00	2
157	-0	.50	3.70	3.00	0.00	3.00	8.00	8.00	1.00	-0.00	-0.00	-0.00	-0.00	2
158	-0	.50	3.00	3.00	0.00	3.00	8.00	8.00	.31	-0.00	-0.00	-0.00	-0.00	2
159	-0	1.10	4.20	3.00	0.00	3.00	8.00	8.00	.51	-0.00	-0.00	-0.00	-0.00	2
160	-0	.50	2.00	2.00	0.00	2.00	8.00	8.00	.50	-0.00	-0.00	-0.00	-0.00	2
161	-0	.50	2.00	2.00	0.00	2.00	8.00	8.00	.37	-0.00	-0.00	-0.00	-0.00	2
162	-0	.70	3.40	2.00	0.00	2.00	8.00	8.00	.22	-0.00	-0.00	-0.00	-0.00	2
163	-0	.50	3.70	2.00	0.00	2.00	8.00	8.00	.41	-0.00	-0.00	-0.00	-0.00	2
164	-0	.50	3.00	2.00	0.00	2.00	8.00	8.00	.36	-0.00	-0.00	-0.00	-0.00	2
165	-0	1.10	4.20	2.00	0.00	2.00	8.00	8.00	.17	-0.00	-0.00	-0.00	-0.00	2
166	-0	.50	2.00	3.68	.10	4.00	8.00	8.00	1.16	-0.00	-0.00	-0.00	-0.00	2
167	-0	.50	2.00	3.68	.10	4.00	8.00	8.00	.36	-0.00	-0.00	-0.00	-0.00	2
168	-0	.70	3.40	3.68	.10	4.00	8.00	8.00	.71	-0.00	-0.00	-0.00	-0.00	2
169	-0	.50	3.70	3.68	.10	4.00	8.00	8.00	.66	-0.00	-0.00	-0.00	-0.00	2
170	-0	.50	3.00	3.68	.10	4.00	8.00	8.00	.15	-0.00	-0.00	-0.00	-0.00	2
171	-0	1.10	4.20	3.68	.10	4.00	8.00	8.00	.30	-0.00	-0.00	-0.00	-0.00	2
172	-0	.50	2.00	2.75	.10	3.00	8.00	8.00	1.34	-0.00	-0.00	-0.00	-0.00	2
173	-0	.50	2.40	2.75	.10	3.00	8.00	8.00	.96	-0.00	-0.00	-0.00	-0.00	2
174	-0	.70	3.40	2.75	.10	3.00	8.00	8.00	1.20	-0.00	-0.00	-0.00	-0.00	2
175	-0	.50	3.70	2.75	.10	3.00	8.00	8.00	.94	-0.00	-0.00	-0.00	-0.00	2
176	-0	.50	3.00	2.75	.10	3.00	8.00	8.00	.72	-0.00	-0.00	-0.00	-0.00	2
177	-0	1.10	4.20	2.75	.10	3.00	8.00	8.00	.33	-0.00	-0.00	-0.00	-0.00	2
178	-0	.50	2.00	1.90	.10	2.00	8.00	8.00	1.82	-0.00	-0.00	-0.00	-0.00	2
179	-0	.50	2.40	1.90	.10	2.00	8.00	8.00	1.63	-0.00	-0.00	-0.00	-0.00	2

Table 1 (Cont'd)

[illegible]

• • • • •

In cases where two side force peaks of nearly equal magnitude are present, the second peak and the angle of attack at which it occurs are noted and included under the headings of  $C'_{ym}$  and  $\alpha'_m$ . The onset angle is taken to be the largest angle of attack at which zero side force is measured. Not all the entries in Table 1 have values for  $\alpha_0$  and  $\alpha_m$ . In some cases these values could not be read clearly, and in others that data was taken from charts showing  $C_{ym}$  only.

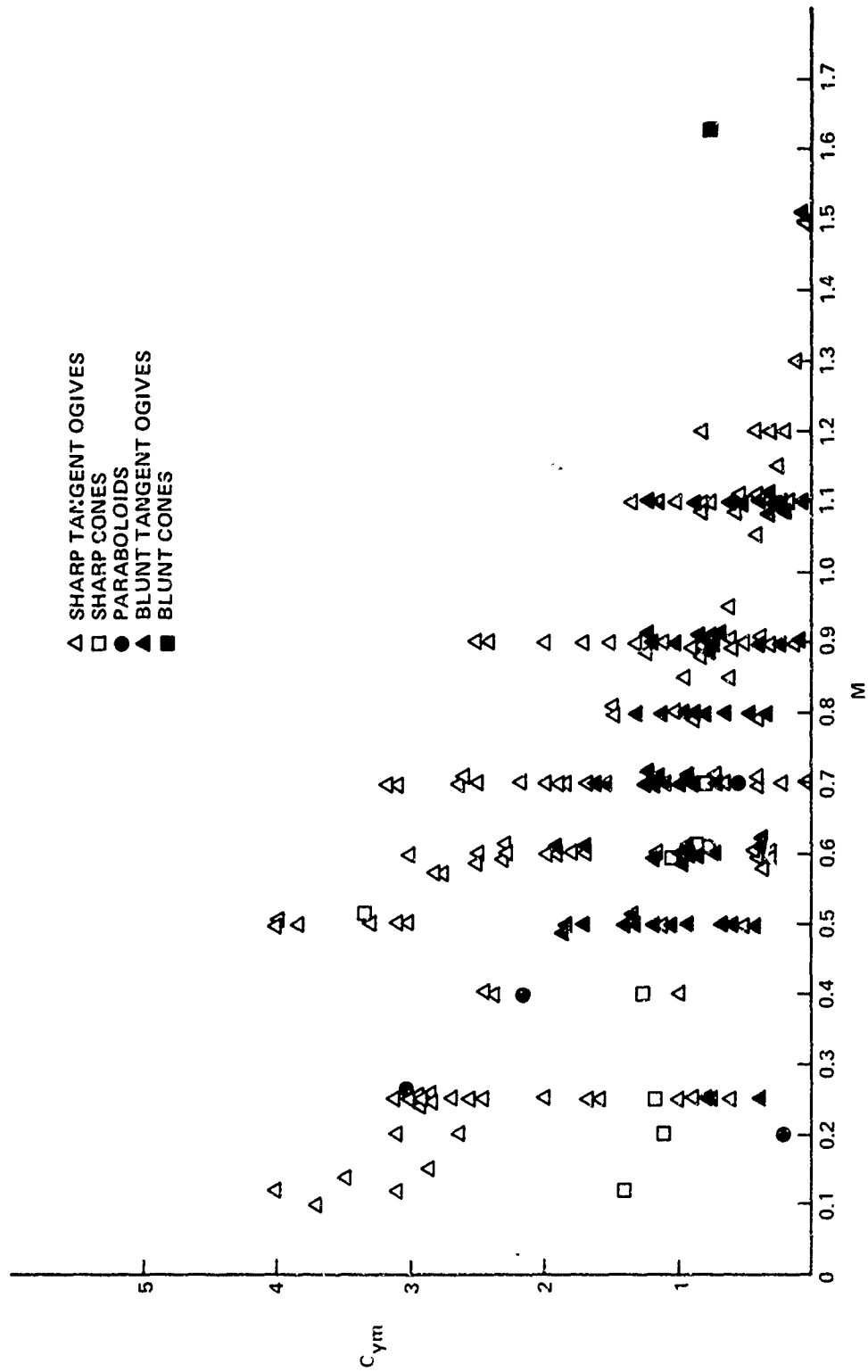
Figures 7 and 8 indicate that  $M$  or  $M_c$  is an important determinant of  $C_{ym}$  particularly in the high subsonic regime where the crossflow Mach number is supercritical. The general trend is for a decreasing value of  $C_{ym}$  with increasing Mach number. Smaller  $l_n$  values result in decreasing values of  $C_{ym}$  as is illustrated in Figure 9. A detailed examination of the data base indicates that this variation is most pronounced at high subsonic Mach numbers. The relation between  $Re$  and  $C_{ym}$  is explored in Figure 10 which suggests a small decrease at higher Reynolds numbers.

The differences in the relations governing blunt and sharp tangent ogive of bodies are seen by examining Figures 7 through 9. Dependencies are much more clearly defined for sharp bodies, particularly for  $l_n$ . The relation between  $C_{ym}$  and  $r_b$  on blunt bodies is shown in Figure 11 and does not indicate a clear trend with variations in nose bluntness.

An examination of Figure 7 shows that significant side forces disappear for  $M > 1.4$ , the only exception being a measurement taken on a cone. Another example is available in the literature showing a small side force on a cone at  $M = 2.25$ . This suggests that cones experience side force to a Mach number higher than do tangent ogives. In Figure 8 it is shown that side force disappears on all classes of bodies for  $M_c > .8$ . Thomson found that at  $M_c \sim .7$  the structure of the leeward flow field changes noticeably with vortices forming only near the body nose and at higher crossflow numbers disappearing altogether.<sup>7</sup>

Examination of the data base indicates that  $\alpha_m$  is related to  $M$  and  $l_T$  while  $\alpha_0$  is a function of  $l_t$  alone. Data for these three relations are presented in Figures 12 through 14, respectively. In all three figures only values of  $\alpha_m$  and  $\alpha_0$  corresponding to cases where  $C_{ym} \geq .75$  are included. An excessive amount of scatter was found in the remaining points due to a difficulty in reading them.

25. Orlik-Rückerman, K. J., La Berge, J. C., Iyengar, S., "Half and Full Model Experiments on Slender Cones at Angle of Attack," Journal of Spacecraft and Rockets, Vol. 11, No. 9, pp. 575-580, Sep 1973.

FIG. 7  $C_{ym}$  AS A FUNCTION OF  $M$  FOR ALL POINTS IN THE DATA BASE.

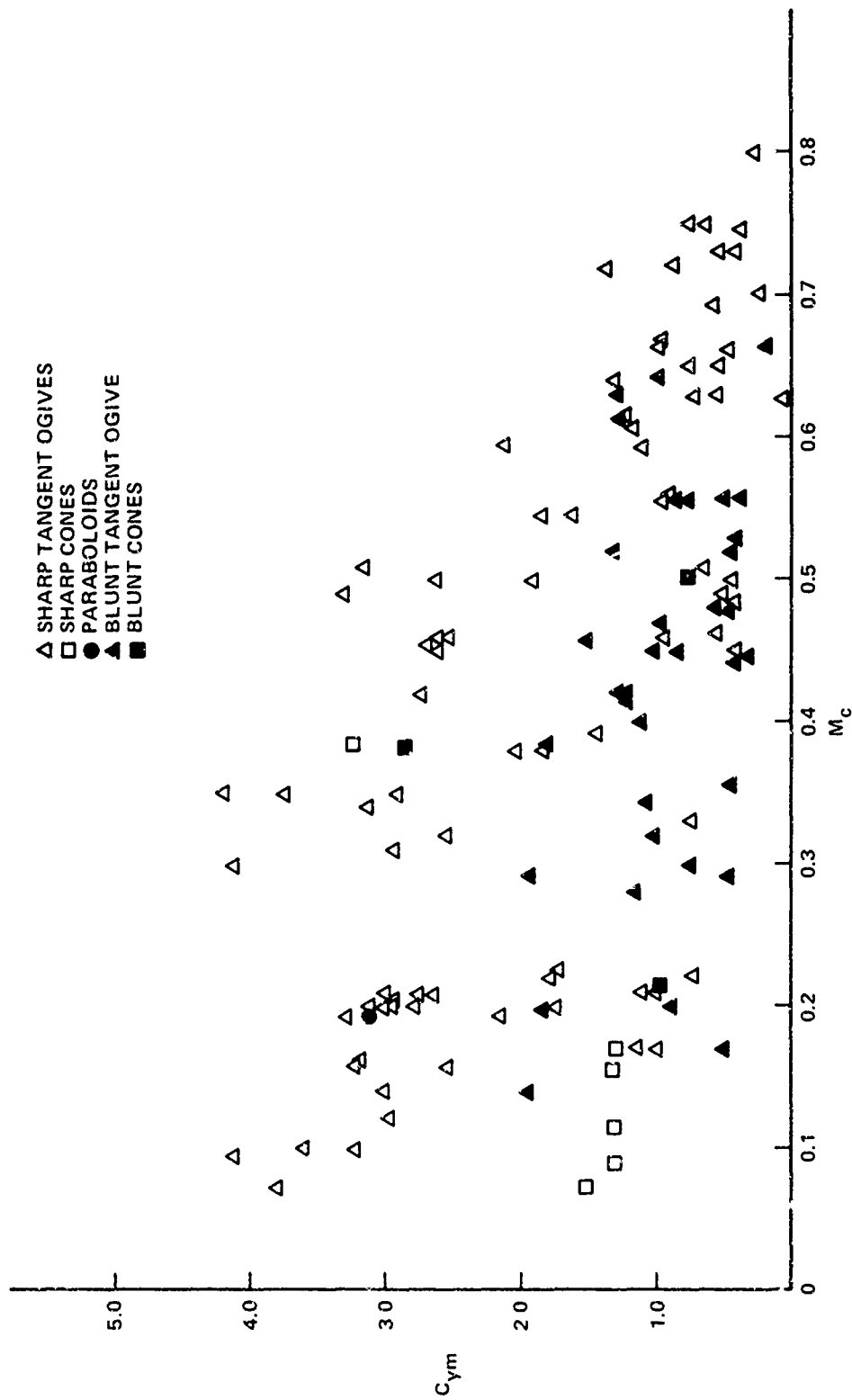
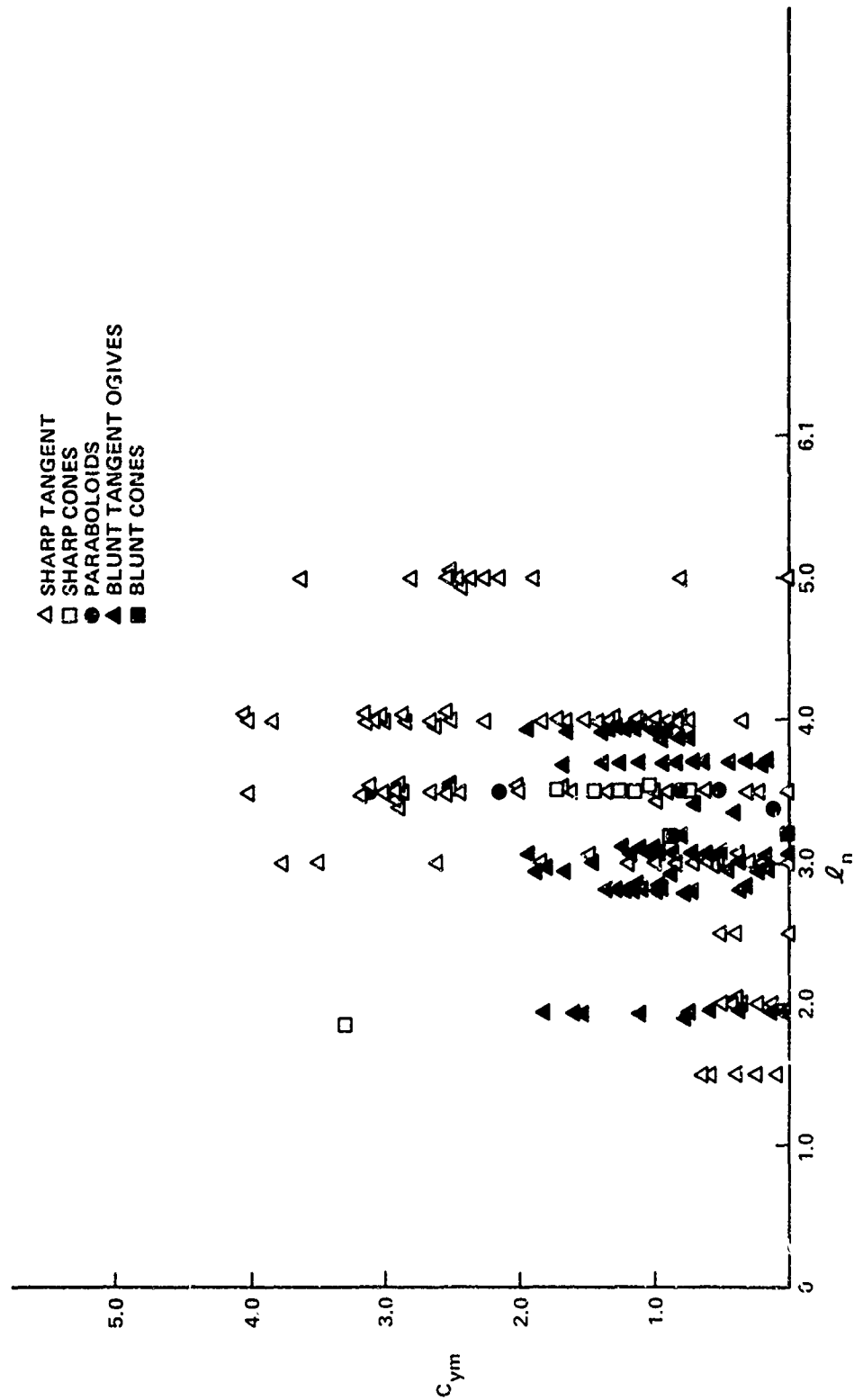
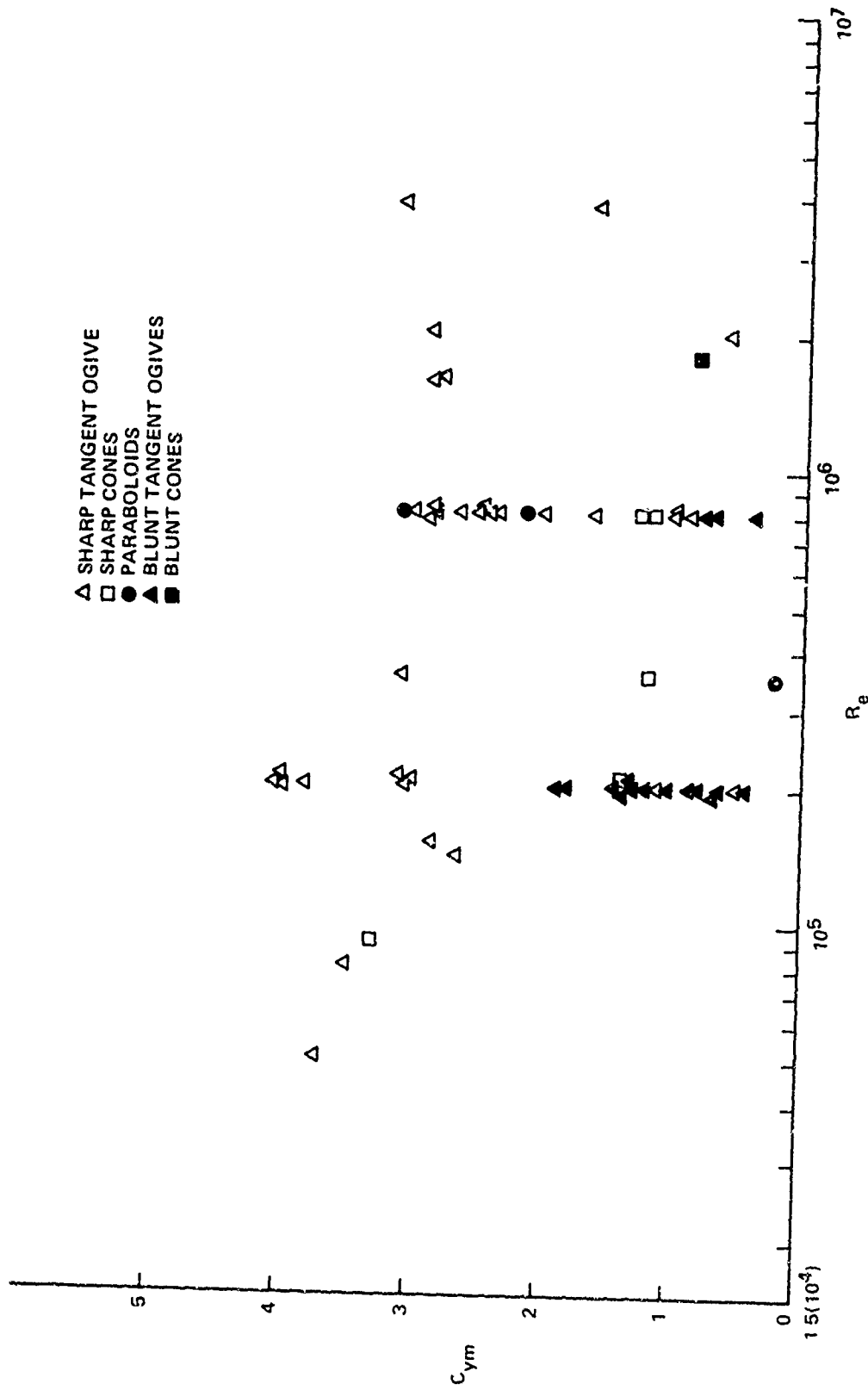


FIG. 3  $C_{ym}$  AS A FUNCTION OF  $M_c = M \sin \alpha_m$  FOR ALL POINTS IN THE DATA BASE FOR WHICH  $\alpha_m$  IS KNOWN.

FIG. 9  $C_{ym}$  AS A FUNCTION OF  $l_n$  FOR ALL POINTS IN THE DATA BASE.

FIG. 10  $C_{ym}$  AS A FUNCTION OF  $R_e$  FOR ALL DATA POINTS HAVING  $M < .51$ .

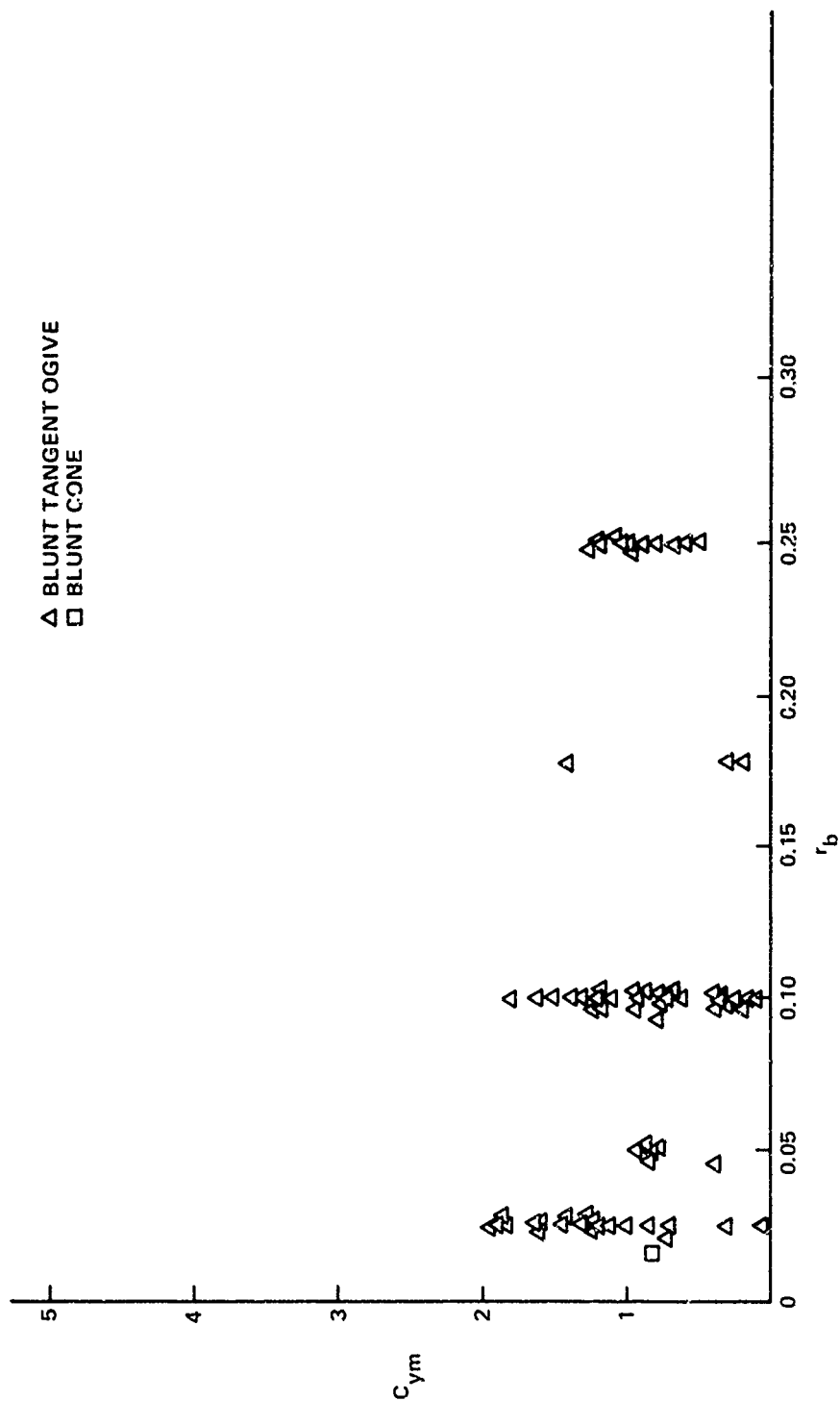


FIG. 11  $C_{ym}$  AS A FUNCTION OF  $r_b$  FOR ALL BLUNT MODELS ( $r_b > 0.005$ ).

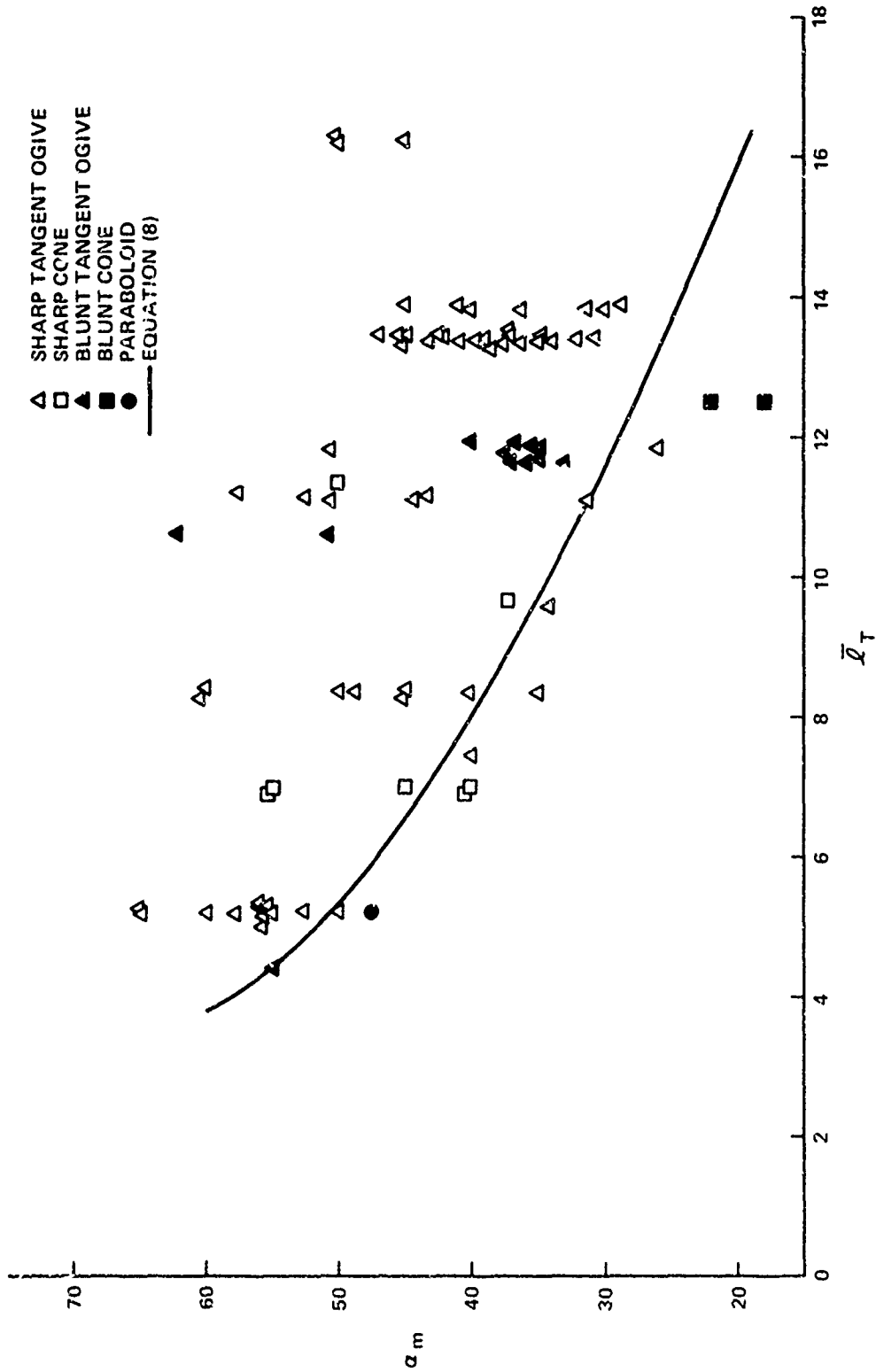
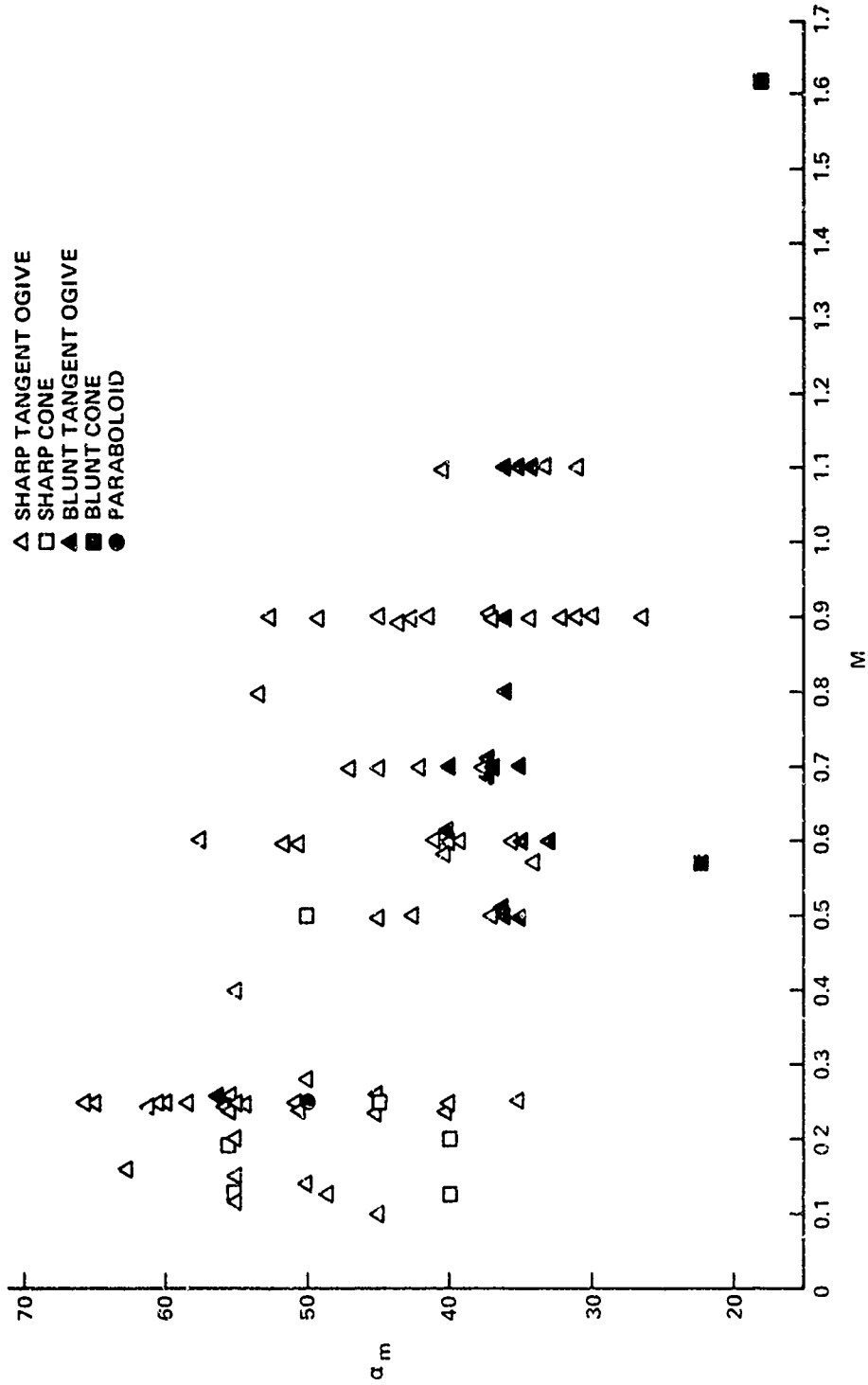


FIG. 12  $\alpha_m$  AS A FUNCTION OF  $\bar{l}_T$  FOR ALL POINTS IN THE DATA BASE WHERE  $\alpha_m$  IS KNOWN AND  $C_{ym} > .75$ . ALSO SHOWN IS EQUATION (8).

FIG 13  $\alpha_m$  AS, FUNCTION M FOR ALL POINTS IN THE DATA BASE WHERE  $\alpha_m$  IS KNOWN AND  $C_{ym} > .75$ .

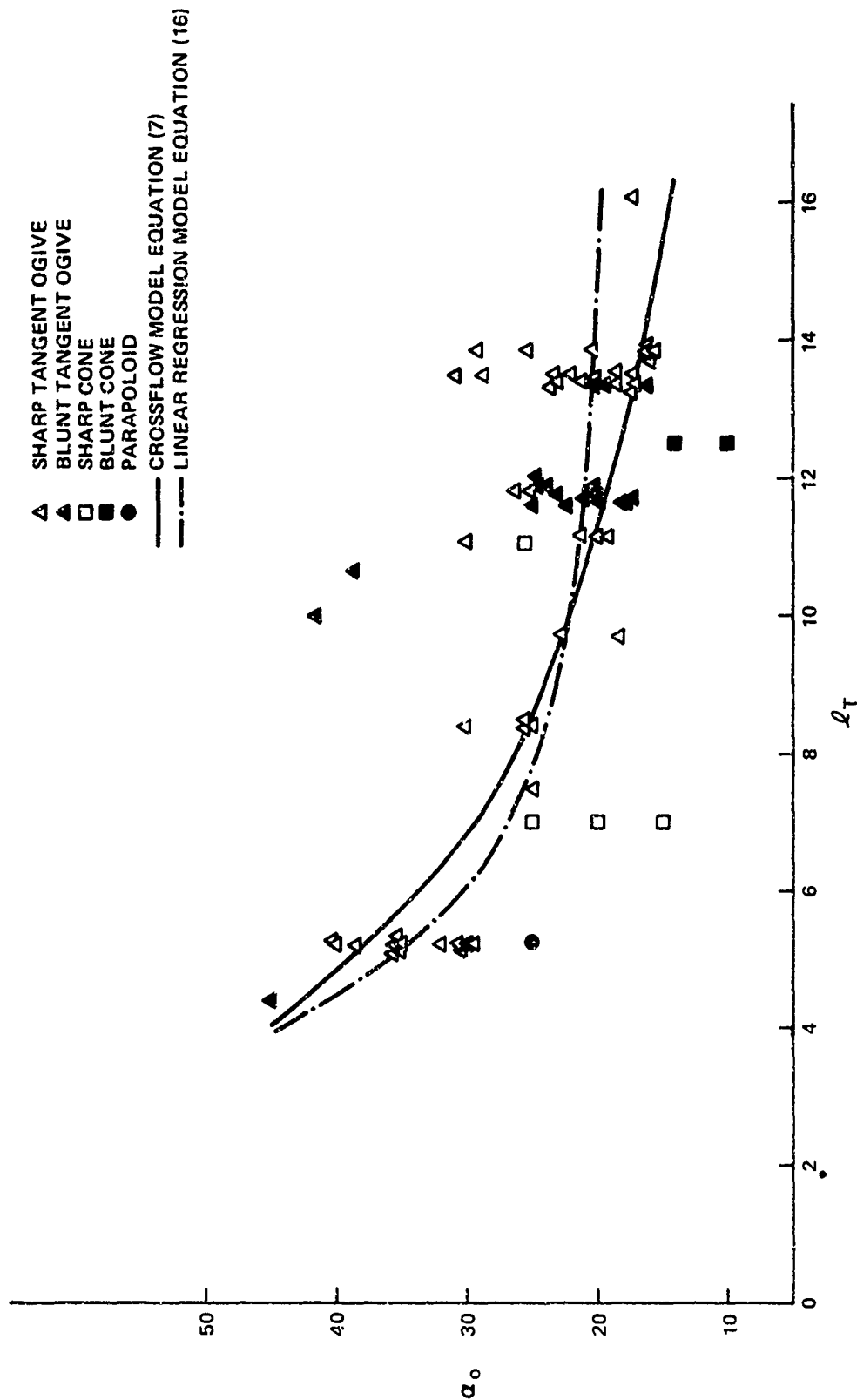


FIG. 14  $\alpha_0$  AS A FUNCTION OF  $l_T$  FOR ALL POINTS IN THE DATA BASE POINTS WHERE  $\alpha_0$  IS KNOWN AND  $C_{ym} > .75$ . ALSO SHOWN IS THE CROSSFLOW MODEL PREDICTION, EQUATION (7), AND THE LINEAR REGRESSION MODEL, EQUATION (8).

## CREATION OF A REGRESSION MODEL

The predictive model is to be developed using Efroymson's multiple regression analysis technique<sup>26</sup>. Once a model has been postulated this method adds terms one by one to the regression equation taking the term with the highest correlation coefficient first. Before this variable is actually included in the model the F test<sup>27</sup> is applied to its variance contribution to determine whether it is statistically significant at a specified F level. At the end of each step, prior to the addition of a new variable, all variables in the model are checked to determine if they are statistically significant and those which are not are dropped.

In order to successfully determine a predictive model using the above algorithm, the correct variables must be included in the proposed set. Although statistically insignificant variables are not incorporated, it is possible for incorrect terms to be included as a result of peculiarities in the data base. Accordingly, in order to develop a predictive equation which is physically reasonable, it is necessary to postulate an initial model which is as accurate as possible.

A model of  $C_{ym}$  is considered first. Consistent with predictions of the crossflow model and the general trends evident in the data base, the following model is assumed:

$$C_{ym} = b_0 + b_1 M + b_2 M^2 + b_3 \frac{1}{I_n} + \frac{b_4}{I_n^2} + b_5 \frac{M}{I_n} + b_6 f(Re) + b_7 r_b + b_8 g\left(\frac{M}{I_t}\right) \quad (9)$$

Here  $f(Re)$  and  $g(r_b)$  are defined as follows:

26. Efroymson, M. A., "Multiple Regression Analysis, Mathematical Methods for Digital Computers," Ralston and Wilt, John Wiley & Sons, New York, 1962, pp. 191-203.
27. Draper, N. R. and Smith, H., "Applied Regression Analysis," John Wiley & Sons, 1966, pp. 24-26.

$$f(Re) = \begin{cases} 0 & Re < 6(10^5) \text{ or } M > .57 \\ 1 & Re > 6(10^5) \text{ and } M < .57 \end{cases}$$

$$q\left(\frac{M}{I_t}\right) = \begin{cases} \frac{M-.57}{I_t} & M > .57 \\ 0 & M < .57 \end{cases}$$

(10)

The form for  $f(Re)$  and  $q\left(\frac{M}{I_t}\right)$  assumed is consistent with the type of

relations suggested by the crossflow model where  $Re$  and  $I_t$  play a very significant role. The variable  $l_n$  has been included in inverted form to insure that in the limit  $l_n \rightarrow \infty$  a finite force is obtained. The parameter  $r_b$  is included since blunting is observed to have a large effect on  $C_{ym}$ .

The data base examination carried out in the preceding section establishes that the type of body has a strong influence on side force. This suggests that a separate model be developed for each class of body, a procedure which is practical in terms of the available data base only for sharp and blunt tangent ogives. The proposed model of Equation (7) is applied to both types of bodies with  $b_7 = 0$  for sharp tangent ogives. Requiring a 95% confidence level<sup>27</sup> for the entering or leaving of a particular variable results in the predictive equation:

(a) Sharp tangent ogives ( $r_b < .005$ )

$$C_{ym} = 4.20 - 12.5 h\left(\frac{M}{I_n}\right) - 1.06 f(Re)$$

Standard Error of  $C_{ym} = .65$  where:

$$h\left(\frac{M}{I_n}\right) = \begin{cases} .3 & \text{for } \frac{M}{I_n} \geq .3 \\ \frac{M}{I_n} & \text{for } \frac{M}{I_n} < .3 \end{cases}$$

(11)

(b) Blunt tangent ogives ( $r_b > .005$ )

$$C_{ym} = 1.17 - .543 f(Re) - 13.91 h'' \left( \frac{M}{l_n} \right)$$

$$\text{Standard Error of } C_{ym} = .380$$

$$h'' = \begin{cases} 0 & M \leq .57 \\ \frac{M-.57}{l_n} & M > .57 \end{cases}$$

(12)

Defining special limits on  $M/l_n$  as described by the functions  $h'$  and  $h''$  were suggested by an examination of the residuals.

As an alternative to Equation (11) a model is proposed using  $M_c$  and  $Re_c$  in place of  $M$  and  $Re$  respectively for tangent ogives. Here again a solution in the form of Equation (7) is assumed with  $b_7 = 0$  and  $f(Re)$  defined as:

$$f(Re) = \begin{cases} 0 & Re_c < 4.25 (10^5) \text{ or } M_c > .5 \\ 1 & Re_c > 4.25 (10^5) \text{ and } M_c < .5 \end{cases}$$

This yields:

$$C_{ym} = 3.65 - 1.019 M_c^2 - 8.39 h \left( \frac{M_c}{l_n} \right) - .889 f(Re)$$

$$\text{Standard Error of } C_{ym} = .70$$

$$h \left( \frac{M_c}{l_n} \right) = \begin{cases} .3 & \frac{M_c}{l_n} \geq .3 \\ \frac{M_c}{l_n} & \frac{M_c}{l_n} \leq .3 \end{cases}$$

(13)

Although this equation does not provide as good a fit as Equation (9), it can be used to generate  $C_{ym}$  as a function of  $\alpha$ .

The variable  $\alpha_m$  is related to  $M$  and  $\bar{l}_t$  by both the crossflow model and the data base. Accordingly the following model is postulated for  $\alpha_m$ :

$$\alpha_m = b_0 + b_1 M + b_2 M^2 + \frac{b_3}{\bar{l}_t} + \frac{b_4}{\bar{l}_t^2} + b_5 \frac{M}{\bar{l}_t} \quad (14)$$

Here again  $\bar{l}_t$  is included in inverted form to yield a finite result in the limit  $l_t \rightarrow \infty$ . The final predictive equation is:

$$\alpha_m = 39.76 - 10.5 M + 91.6/\bar{l}_t$$

$$\text{standard error of } \alpha_m = 6.95$$

(15)

Only  $\alpha_m$  corresponding to  $C_{ym} > .75$  are represented in this equation for the previously mentioned reasons, and for data having two  $C_{ym}$  peaks, both are used.

The variable  $\alpha_o$  is related to  $\bar{l}_t$  by both the data base and the crossflow model. Accordingly, the following predictive equation is proposed:

$$\alpha_o = b_o + \frac{b_1}{\bar{l}_t} + \frac{b_2}{\bar{l}_t^2} + \frac{b_3}{\bar{l}_t^3} \quad (16)$$

which yields:

$$\alpha_o = 18.22 + \frac{425.7}{\bar{l}_t^2} \quad \text{standard error of } \alpha_o = 4.75$$

#### COMPARISON OF REGRESSION AND CROSSFLOW MODEL

The crossflow model for  $C_{ym}$  differs significantly from the final regression equations. Although both approaches indicate that  $M$  is an important variable, the critical model dimension is  $l_n$ , not  $l_t$  as suggested by the crossflow approach. Also, on sharp tangent ogives peak  $C_y$  values are three to four times larger than the crossflow model predictions and only a weak Reynolds number effect is noted. These differences suggest that  $C_{ym}$  values are a product of the flow about the model nose. The expanding body radius in the nose region produces a favorable pressure gradient retarding the formation of a turbulent boundary layer and reducing the  $Re$  effect. To correctly

model  $C_{ym}$ ,  $C_L$  values should be used which correspond to the initial ones following the start of impulsive flow about an expanding cylinder. Such experimental information is currently not available.

The prediction of the crossflow model for  $\alpha_0$  closely corresponds to the results of the linear regression model as is shown in Figure 14. Both approaches define  $\alpha_0$  as a function of  $\bar{l}_t$  which decreases with increasing value of this variable. This good agreement indicates that the onset of side forces occurs in a manner which is consistent with the crossflow model.

The crossflow model and the regression equations both indicate that  $\alpha_m$  is a function of  $\bar{l}_t$  and  $M$ , decreasing as either of these variables increases. The importance of  $\bar{l}_t$  in the regression model is unexpected since  $l_n$  is the critical model dimension in determining  $C_{ym}$ . This can be understood by noting that  $\alpha_m > \alpha_0$  and  $\alpha_0$  varies extensively with  $\bar{l}_t$ . The physical significance of the Mach number dependency for  $\alpha_m$  is clearly explained by the crossflow model which indicates that  $C_L$  and hence  $C_y$  decreases as  $M_c$  increases towards the transonic regime. Hence, for  $M$  near or greater than unity,  $C_{ym}$  must occur at low  $\alpha$  to insure that  $M_c$  is small.

The solution for  $\alpha_f$  as defined by Equation (8) is plotted in Figure 12. This quantity represents the minimum angle of attack at which a complete cell is present on body. As can be seen from this graph, it seems to define a lower bound for  $\alpha_m$ .

### CONCLUSIONS

A detailed examination of the data base leads to the following conclusions:

- (a) Cones, sharp tangent ogives, and blunt tangent ogives all show different side force characteristics.
- (b) In all cases  $C_{ym}$  decreases with increasing  $M$  and disappears for  $M > 1.4$  on tangent ogives and  $M > 2.0$  on cones.
- (c) On tangent ogives  $C_{ym}$  decreases with increasing  $l_n$  particularly in the case of sharp bodies.
- (d) Blunt tangent ogives show a lower level of  $C_{ym}$  than sharp ones, but the degree of bluntness does not appear important.
- (e) The onset angle,  $\alpha_0$ , decreases with increasing  $\bar{l}_t$ .
- (f) The parameter  $\alpha_m$  decreases with increasing  $M$  and  $\bar{l}_t$ .

The final regression equations incorporate the above observations and in addition suggest the following which is motivated by the crossflow model predictions.

(g) On tangent ogives,  $C_{ym}$  is a weak function of  $Re$ , decreasing under the conditions of turbulent separation at subcritical Mach numbers.

This last conclusion should be considered as tentative. Most of the high  $Re$  points are from a single facility and the supposed  $Re$  influence may possibly be a facility effect.

Comparison of the linear regression equations with the crossflow model predictions suggests that the peak loads on sharp bodies are associated with the flow about the body nose. This conclusion is based on the observation that  $l_n$  is the critical dimension in the regression model and plays a role similar to  $l_t$  in the crossflow model. The good agreement between regression and crossflow models for  $\alpha_0$  indicate that side forces arise in a manner which is consistent with the crossflow theory.

The linear regression equations for  $C_{ym}$ ,  $\alpha_0$ , and  $\alpha_m$  developed in this report provide for the first time a method of estimating values for these parameters. These specific equations, which should be updated when a more comprehensive data base becomes available, are a product and not a part of the papers theme. The central idea is that realistic prediction methods for bodies at high angles of attack in the subsonic-transonic range must take into account the nondeterministic nature of the flowfield. The load on and hence, the flowfield about bodies under these conditions will fluctuate for reasons which are difficult to identify and often not practical to control. Conclusions concerning the characteristics of side force cannot be drawn from a limited number of tests, but can only be determined in a statistical sense by considering a large number of measurements. However, a physical understanding of the phenomena is essential for the development of an optimum predictive model.